

# Mathematical Analysis of Spontaneous Emergence of Cell Polarity

Wing-Cheong Lo · Hay-Oak Park ·  
Ching-Shan Chou

Received: 13 September 2013 / Accepted: 23 May 2014 / Published online: 15 July 2014  
© Society for Mathematical Biology 2014

**Abstract** Cell polarization, in which intracellular substances are asymmetrically distributed, enables cells to carry out specialized functions. While cell polarity is often induced by intracellular or extracellular spatial cues, spontaneous polarization (the so-called symmetry breaking) may also occur in the absence of spatial cues. Many computational models have been used to investigate the mechanisms of symmetry breaking, and it was proved that spontaneous polarization occurs when the lateral diffusion of inactive signaling molecules is much faster than that of active signaling molecules. This conclusion leaves an important question of how, as observed in many biological systems, cell polarity emerges when active and inactive membrane-bound molecules diffuse at similar rates while cycling between cytoplasm and membrane takes place. The recent studies of Rätz and Röger showed that, when the cytosolic and membrane diffusion are very different, spontaneous polarization is possible even if the membrane-bound species diffuse at the same rate. In this paper, we formulate a two-equation non-local reaction-diffusion model with general forms of positive feedback. We apply Turing stability analysis to identify parameter conditions for achieving cell polarization. Our results show that spontaneous polarization can be achieved within some parameter ranges even when active and inactive signaling molecules diffuse at similar rates. In addition, different forms of positive feedback are explored to show

---

W.-C. Lo (✉)

Mathematical Biosciences Institute, The Ohio State University, Columbus, OH 43210, USA  
e-mail: lo.75@mbi.osu.edu

H.-O. Park

Department of Molecular Genetics, The Ohio State University, Columbus, OH 43210, USA

C.-S. Chou

Department of Mathematics, The Ohio State University, Columbus, OH 43210, USA

that a non-local molecule-mediated feedback is important for sharpening the localization as well as giving rise to fast dynamics to achieve robust polarization.

**Keywords** Cell polarization · Turing stability analysis · Budding yeast · Non-local feedback

## 1 Introduction

Cell polarization, in which substances previously uniformly distributed become asymmetrically localized, is fundamental to various cellular processes such as differentiation, migration, and development. Failure in polarization may lead to lethality or dysfunctionality of the cells. How cell polarity is established and maintained has been a central question in cell biology. The fundamental mechanisms for cell polarization remain controversial, but it is known that polarity development typically involves the localization of signaling molecules to a proper location of the cell membrane (Bryant and Mostov 2008), which can be exemplified by the localization of PAR proteins (Goldstein and Macara 2007), Scribble proteins (Humbert et al. 2003), phosphoinositide lipids (Krahn and Wodarz 2012), and Rho family GTPase (Raftopoulou and Hall 2004). These signaling molecules are initially distributed in the cytoplasm, and then, in response to extracellular or intracellular cues, they are finally localized at a proper location on the plasma membrane. The localization of signaling molecules activates certain cellular pathways, and ultimately leads to the organization of the cytoskeleton or other responses, which contributes to cell morphogenesis or motility.

The budding yeast *Saccharomyces cerevisiae* has been an excellent model system to study cell polarization owing to simple, yet powerful experimental tools available in this organism. In yeast cell, a new daughter cell emerges from the original (mother) cell, referred to as budding, and this is a result of cell polarization at the bud site. In wild-type cells, the selection of a bud site is determined by spatial cues that are distinct in each cell type. However, most previous works have studied polarization in the absence of these spatial cues (Park and Bi 2007; Slaughter et al. 2009) by deleting a crucial molecule, Rsr1, which links the spatial cue and the downstream polarization machinery. As a result, the cells will choose their bud sites in a fully random and spontaneous manner, which is the so-called symmetry breaking. This symmetry breaking is not unique to yeast, but can also be observed in mammalian neutrophils and amoeba (Drubin and Nelson 1996; Wedlich-Soldner and Li 2003). To understand the mechanisms underlying symmetry breaking, several mathematical models have been proposed, which can roughly be categorized into two groups. The first type is deterministic models, that is, reaction-diffusion equations. In those models, Turing-type mechanism was suggested to be responsible for the self-organization of molecules which gives rise to cell polarity (Goryachev and Pokhilko 2008; Jilkine and Edelstein-Keshet 2011; Rätz and Röger 2012). The second type is stochastic models in which individual molecular interactions are considered (Altschuler et al. 2008; Freisinger et al. 2013). Though from different perspectives, both continuum and stochastic models emphasize the importance of cycling of GTP and GDP bound forms of the polarized protein Cdc42 (we will refer them as active and inactive forms, respectively) and the

Bem1- or Rdi1-mediated positive feedback that further accelerates the recruitment and activation of Cdc42. In particular, [Altschuler et al. \(2008\)](#) have shown that an intrinsic stochastic mechanism through linear positive feedback alone is sufficient to account for the spontaneous establishment of a single site of polarity, but the same linear positive feedback is not sufficient for symmetry breaking in deterministic models, which suggests a fundamental difference between stochastic and deterministic models. On the other hand, this conclusion raises interesting questions: why does linear positive feedback fail to work in deterministic model? Is there a mathematical explanation? What would be the general “admissible” forms of positive feedback which give rise to robust cell polarization? In this paper, we attempt to use mathematical analysis to address the above questions and propose possible mechanisms through which the feedback is established.

In previous works ([Goryachev and Pokhilko 2008](#); [Jilkiné and Edelstein-Keshet 2011](#); [Rätz and Röger 2012](#)) concerning Turing-type mechanism for cell polarization, numerical simulations have been performed to investigate the parameters, but conditions for Turing instability, therefore cell polarization, are not studied in detail. By considering the cytoplasmic and membrane-bound inactive species as one pooled variable, and the membrane-bound active species as the other variable, usually assuming the ratio of the diffusion rates of these two is large, stability analysis has been performed ([Rätz and Röger 2012](#); [Rubinstein et al. 2012](#)). In the recent work, [Rätz and Röger \(2012\)](#) presented a non-local reaction-diffusion model and performed a Turing stability analysis to study the conditions for achieving Turing instability. They reach the conclusion that Turing instability occurs when the lateral diffusion of inactive signaling molecules is much faster than that of active signaling molecules. In [Rubinstein et al. \(2012\)](#), the authors performed weakly nonlinear analysis to a similar system to obtain information about the dynamics of the solution. There are also models which separate the membrane-bound species and cytosolic species in different domains, with the communication of molecules between these two domains represented by fluxes ([Levine and Rappel 2005](#); [Rätz and Röger 2013](#)). In [Rätz and Röger \(2013\)](#), linear stability analysis was performed for this type of model, with two possible mechanisms of cell polarization were identified: Turing stability or polarization induced by the difference in cytosolic and lateral diffusion. This result supports that spontaneous polarization is possible even when lateral diffusion coefficients are same and the biochemical network in [Rätz and Röger \(2013\)](#) has been applied for studying cell motility ([Marth and Voigt 2013](#)). In many biological systems, the membrane-bound active and inactive signaling molecules diffuse at similar rates, while the inactive form cycles between the cytoplasm and membrane, for example, Cdc42 molecules in budding yeast ([Goryachev and Pokhilko 2008](#); [Lo et al. 2013](#)). It is important to know whether Turing instability occurs in that case. In this paper, we formulate a non-local reaction-diffusion model with two membrane-bound species and general forms of positive feedback. Turing stability analysis ([Turing 1990](#)) is applied to identify parameter conditions for achieving cell polarization. Our analysis shows that Turing instability indeed exists when active and inactive signaling molecules have the same diffusion rates. Also, different forms of positive feedback are explored to show the relationship between feedback function forms and the robustness of cell polarization.

This paper is organized as follows. In Sect. 2, we present a two-equation reaction-diffusion model of cell polarization with a general function form of positive feedback. In Sect. 3, we perform Turing stability analysis to the model proposed in Sect. 2 to derive conditions for which cell polarity emerges. Sections 4 and 5 contain the discussion of different forms of positive feedback which lead to different localization patterns. In Sect. 6, we show that a robust polarization can be achieved through non-local positive feedback and that the polarization is tight. Finally, conclusion is presented in Sect. 7.

## 2 A Two-Equation Model for Cell Polarization

Cell polarization can be generally simplified as processes involving exchange of active and inactive forms of polarized molecules, feedbacks through molecular interactions, as well as physical mechanisms such as transport and diffusion. Reaction-diffusion mathematical models have been widely used to model cell polarization for different biological systems, and these models have led to proposed mechanisms such as wave pinning (Jilkine et al. 2007; Maree et al. 2006) and Turing instability (Goryachev and Pokhilko 2008; Turing 1990) to explain how robust localization of molecules forms in the presence of cytoplasmic or membrane diffusion. Despite the differences among various previous models for the emergence of cell polarity, all these models include a positive feedback mechanism, mediated through either chemical interactions with other species or physical transport.

In this paper, we consider a continuum mathematical model describing the dynamics of a polarized signaling molecule on the cell membrane: the variables include its active and inactive *membrane-bound* forms (we use the term “active form” to indicate that only this form is functional to induce the downstream cellular responses, although the “inactive” molecules are also important in the cycling of molecules). The cytoplasmic inactive form of this molecule is also involved, but it is modeled implicitly through conservation of total molecules. This type of polarized molecules can be well exemplified by Cdc42-GTPase cycle in budding yeast, with Cdc42-GDP its inactive form and Cdc42-GTP its active form. Most of the GTPase cycles have a common mechanism that enables them to switch between the active (GTP-bound) and inactive (GDP-bound) states. The switch from inactive to active is initiated by hydrolysis and it can be reversed by guanine nucleotide exchange factors (GEFs), which cause the GDP to dissociate from the GTP. When the GDP is bound, GDIs bind to the GTPase and release the GDP from the cell membrane to the cytoplasm. This process can be reversed by the action of a GDI displacement factor.

The domain in our model could be the membrane of a cell, which is a sphere, or for simplicity it could be the cross section of the cell, which is a circle. The domain is denoted by  $M$ , which is either a circle (one-dimensional domain) or a spherical surface (two-dimensional domain). We use  $a$  and  $b$  to represent active and inactive membrane-bound signaling molecules, respectively; without confusion in the context, we will also use  $a$  and  $b$  to denote their corresponding particle fractions, which is unitless (Altschuler et al. 2008). Thus, the exact partial numbers of active and inactive signaling molecules in any open subset  $A$  of the domain  $M$  can be calculated by

$$N_{aA} = \frac{N}{|M|} \int_A a \, dS \text{ and } N_{bA} = \frac{N}{|M|} \int_A b \, dS,$$

where  $|M|$  equals to the total area of the domain  $M$ , and  $N$  is the total number of active and inactive signaling molecules in the whole cell including membrane and cytoplasm.

The dynamics of  $a$  and  $b$  are thus governed by a reaction–diffusion system, which may be non-local depending on the function form of  $F(\cdot, \cdot)$ :

$$\frac{\partial a}{\partial t} = D_m \nabla^2 a + F(a, \hat{a}^n) b - k_{\text{off}} a, \tag{1}$$

$$\frac{\partial b}{\partial t} = D_m \nabla^2 b - F(a, \hat{a}^n) b + k_{\text{off}} a + g_{\text{on}}(1 - \hat{a} - \hat{b}) - g_{\text{off}} b, \tag{2}$$

with  $\hat{a}^n = \int_M a^n \, dS/|M|$ ,  $\hat{a} = \int_M a \, dS/|M|$  and  $\hat{b} = \int_M b \, dS/|M|$  respectively representing the average values of  $a^n$ ,  $a$  and  $b$  over the cell membrane. In this paper, two kinds of spatial domain are considered: (1) one-dimensional cross section of the cell membrane of radius  $R \, \mu\text{m}$ , as in Fig. 1a; (2) two-dimensional spherical surface of the cell membrane of radius  $R \, \mu\text{m}$ . Periodic boundary conditions are used for both domains.

The first terms of the right-hand side in Eqs. (1) and (2) represent the diffusion of species  $a$  and  $b$  with  $D_m$  the lateral surface diffusion rate and  $\nabla^2$  the Laplacian operator on the cell membrane. In many systems such as budding yeast, it is reasonable to assume that the membrane diffusion rates of active (Cdc42-GTP) and inactive (Cdc42-GDP) signaling molecules are approximately the same (Lo et al. 2013; Goryachev and Pokhilko 2008), and therefore we take the same value  $D_m$  for both species.

In our model, a key assumption is that the total number of active and inactive signaling molecules in the whole cell is conserved. Along with the fact that  $\hat{a}$  and  $\hat{b}$  represent the total fractions of the membrane-bound species, we obtain

$$N = N(\hat{a} + \hat{b} + \text{Frac}_c), \tag{3}$$

where  $\text{Frac}_c$  stands for the fraction of cytoplasmic signaling molecules. Hence, by (3),  $\text{Frac}_c = 1 - \hat{a} - \hat{b}$ . Under the assumption that signaling molecules are uniformly distributed throughout the cytoplasm due to fast cytoplasmic diffusion and the recruitment rate is proportional to the fraction of cytoplasmic signaling molecules,  $g_{\text{on}}(1 - \hat{a} - \hat{b})$  is the recruitment rate of the inactive molecules from the cytoplasm to the membrane. We remark here that to ensure  $1 - \hat{a} - \hat{b}$  being between 0 and 1 to represent the fraction, the initial value for  $\hat{a} + \hat{b}$  needs to be less than 1, which is assumed throughout this paper. The last term in Eq. (2),  $g_{\text{off}} b$ , is the rate at which membrane-bound signaling molecules are extracted into the cytoplasm. The constant  $k_{\text{off}}$  is the deactivation rate coefficient of signaling molecules from active form to inactive form.

In Eqs. (1)–(2), the function  $F$  represents the activation rate for signaling molecules. By assuming that active signaling molecules form a feedback loop to promote activation, meaning that the activation from the inactive form ( $b$ ) to the active form

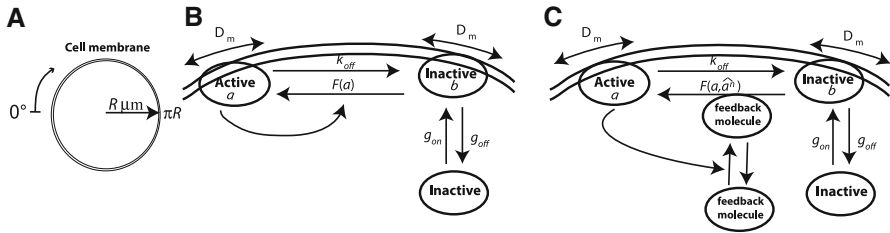


**Fig. 1** One-dimensional spatial domain and two forms of positive feedback in the cell polarization model. Variables and parameters are as in model (1)–(2). **a** Simplified one-dimensional spatial domain represents the cross section of the cell membrane of radius  $R \mu\text{m}$ ; **b** molecule interactions with a local positive feedback (4); **c** molecule interactions with a non-local positive feedback (5)

( $a$ ) is positively regulated by the active molecules ( $a$ ), the function  $F$  is thus positively correlated with the particle density of  $a$ . In this paper, we consider two different feedback functions:

$$F(a) = k_{11} + k_{12}a^n; \tag{4}$$

and

$$F(a, \hat{a}^n) = k_{\text{on}} \frac{k_{21} + k_{22}a^n}{1 + k_{21} + k_{22}\hat{a}^n}. \tag{5}$$

The first function form in Eq. (4) is a direct cooperative feedback which only depends on the local values of  $a$ . This feedback process includes multi-step cooperative interactions such as recruitment and binding. This nonlinear cooperativity is modeled by the  $a^n$ , with  $n \geq 1$ , and  $n$  stands for the degree of cooperativity and is called the cooperativity coefficient. This type of feedback has been used in many Turing type systems (Meinhardt 1982; Turing 1990). The parameter  $k_{11}$  represents the basal activation rate of Cdc42 and the parameter  $k_{12}$  represents the activation rate coefficient through the cooperative feedback. The second function form in Eq. (5) involves a non-local term  $\hat{a}^n$ , as well as the local density  $a$ . This function models feedback that is mediated through another species initially uniformly distributed in the cytoplasm, as in Goryachev and Pokhilko (2008), Lo et al. (2013). A good example is the well-known positive feedback of Cdc42-GTP mediated by the Bem1 complex in budding yeast. Other than Bem1 complex, Smith et al. (2013) proposed that Rdi1, the Cdc42 guanine nucleotide dissociation inhibitor, plays a critical role for symmetry breaking. Similar to Bem1 complex, Rdi1 is initially uniformly distributed in the cytoplasm and forms a Rdi1-Cdc42 complex which enhances Cdc42 localization on the membrane. The detailed derivation of this feedback will be discussed in Sect. 6. These two forms of positive feedback are illustrated in Fig. 1b and c, with the corresponding interactions and parameters in model (1)–(2).

### 3 Linear Stability Analysis

In this section, we apply Turing stability analysis Turing (1990) to study the conditions of the parameters to achieve spontaneous cell polarization. We remark here that the stability analysis in this section can be applied for general feedback function  $F(a, \hat{a}^n)$ .

First, we study a homogeneous steady state solution  $(a_0, b_0)$  of the system (1)–(2), which satisfies the following equations:

$$0 = F(a_0, a_0^n)b_0 - k_{\text{off}}a_0, \tag{6}$$

$$0 = -F(a_0, a_0^n)b_0 + k_{\text{off}}a_0 + g_{\text{on}}(1 - a_0 - b_0) - g_{\text{off}}b_0. \tag{7}$$

Note that since  $a_0$  is homogeneous over space,  $\widehat{a_0^n} = a_0^n$ ,  $\widehat{a_0} = a_0$ , and  $\widehat{b_0} = b_0$ . By summing up (6) and (7), we obtain

$$0 = g_{\text{on}}(1 - a_0 - b_0) - g_{\text{off}}b_0,$$

and hence

$$b_0 = \frac{g_{\text{on}}}{g_{\text{on}} + g_{\text{off}}}(1 - a_0). \tag{8}$$

By substituting (8) into (6), we have

$$0 = \frac{g_{\text{on}}}{g_{\text{on}} + g_{\text{off}}}F(a_0, a_0^n)(1 - a_0) - k_{\text{off}}a_0. \tag{9}$$

When  $a_0 = 1$ , the right-hand side of (9) is negative; when  $a_0 = 0$ , the right-hand side of (9) is positive ( $F$  is a positive function because it represents positive feedback). By the intermediate value theorem, at least one homogeneous steady state solution  $a_0$  exists between 0 and 1, and then by (8), a corresponding non-negative homogeneous steady state solution  $b_0$  can be found.

To examine the stability of a homogeneous steady state solution with respect to small perturbations, we define  $a(x, t)$  and  $b(x, t)$  as slightly perturbed functions from the homogeneous steady state:

$$a(x, t) = a_0 + \epsilon a_1(x, t), \tag{10}$$

$$b(x, t) = b_0 + \epsilon b_1(x, t), \tag{11}$$

where the perturbation amplitude  $\epsilon \ll 1$  is much smaller than  $a_0$  and  $b_0$ . After substituting (10) and (11) into the model (1)–(2) and applying Taylor expansion around  $(a_0, b_0)$ , the leading terms satisfy the following system:

$$\begin{aligned} \frac{\partial a_1}{\partial t} = & D_m \nabla^2 a_1 + (F_{X_1}(a_0, a_0^n)a_1 + na_0^{n-1}\widehat{a_1}F_{X_2}(a_0, a_0^n))b_0 - k_{\text{off}}a_1 \\ & + F(a_0, a_0^n)b_1, \end{aligned} \tag{12}$$

$$\begin{aligned} \frac{\partial b_1}{\partial t} = & D_m \nabla^2 b_1 - (F_{X_1}(a_0, a_0^n)a_1 + na_0^{n-1}\widehat{a_1}F_{X_2}(a_0, a_0^n))b_0 + k_{\text{off}}a_1 \\ & - F(a_0, a_0^n)b_1 - g_{\text{on}}\widehat{a_1} - g_{\text{on}}\widehat{b_1} - g_{\text{off}}b_1, \end{aligned} \tag{13}$$

where  $F_{X_1}$  and  $F_{X_2}$  denote the partial derivatives with respect to the first and the second arguments, respectively. We note that when the local feedback function (4) is considered,  $F_{X_1}$  is positive and  $F_{X_2}$  equals to zero; when the non-local feedback function (5) is considered,  $F_{X_1}$  is positive and  $F_{X_2}$  is negative.

Here we consider a particular spatially periodic perturbation

$$a_1(x, t) = \alpha e^{\lambda t} E_k(x),$$

$$b_1(x, t) = \beta e^{\lambda t} E_k(x),$$

where  $\alpha$  and  $\beta$  are nonzero parameters,  $k$  is a non-negative integer, and  $E_k(x)$  is the  $k$ th non-zero eigenfunction of Laplace operator. System (12)–(13) becomes

$$\lambda \begin{pmatrix} \alpha \\ \beta \end{pmatrix} = \begin{pmatrix} -\sigma_k D_m + (F_{X_1} + \delta(k)na_0^{n-1}F_{X_2})b_0 - k_{\text{off}} & F \\ -(F_{X_1} + \delta(k)na_0^{n-1}F_{X_2})b_0 + k_{\text{off}} - \delta(k)g_{\text{on}} & -\sigma_k D_m - F - \delta(k)g_{\text{on}} - g_{\text{off}} \end{pmatrix} \begin{pmatrix} \alpha \\ \beta \end{pmatrix}, \tag{14}$$

where

$$\delta(k) = \begin{cases} 1 & \text{if } k = 0, \\ 0 & \text{if } k > 0, \end{cases}$$

and the eigenvalue

$$\sigma_k = \begin{cases} k^2/R^2 & \text{for a one-dimensional cross section,} \\ 2k^2/R^2 & \text{for a two-dimensional spherical surface,} \end{cases}$$

where  $R$  is the radius of the circle or sphere, and  $F_{X_1}, F_{X_2}, F$  are evaluated at  $(a_0, a_0^n)$ . It is worth to make a remark that all the analysis can be applied for two-dimensional smooth ellipsoid surface (not necessarily spherical surface) by considering corresponding eigenvalues and eigenfunctions of Laplace operator.

If we define

$$\mathbf{J} = \begin{pmatrix} -\sigma_k D_m + (F_{X_1} + \delta(k)na_0^{n-1}F_{X_2})b_0 - k_{\text{off}} & F \\ -(F_{X_1} + \delta(k)na_0^{n-1}F_{X_2})b_0 + k_{\text{off}} - \delta(k)g_{\text{on}} & -\sigma_k D_m - F - \delta(k)g_{\text{on}} - g_{\text{off}} \end{pmatrix},$$

then Eq. (14) becomes

$$\mathbf{J} \begin{pmatrix} \alpha \\ \beta \end{pmatrix} = \lambda \begin{pmatrix} \alpha \\ \beta \end{pmatrix}. \tag{15}$$

Therefore,  $\lambda$  is an eigenvalue of  $\mathbf{J}$ , and  $(\alpha, \beta)^T$  is the corresponding eigenvector. Eq. (15) has a nonzero solution  $(\alpha, \beta)$  if and only if  $\det(\mathbf{J} - \lambda \mathbf{I}) = 0$ , which means that  $\lambda$  should be a zero of the following characteristic polynomial:

$$\lambda^2 - \lambda \left( -2\sigma_k D_m + (F_{X_1} + \delta(k)na_0^{n-1}F_{X_2})b_0 - k_{\text{off}} - F - \delta(k)g_{\text{on}} - g_{\text{off}} \right) + \sigma_k^2 D_m^2 - \sigma_k D_m \left( (F_{X_1} + \delta(k)na_0^{n-1}F_{X_2})b_0 - k_{\text{off}} - F - \delta(k)g_{\text{on}} - g_{\text{off}} \right)$$



$$- (\delta(k)g_{\text{on}} + g_{\text{off}})((F_{X_1} + \delta(k)na_0^{n-1}F_{X_2})b_0 - k_{\text{off}}) + F\delta(k)g_{\text{on}} = 0. \tag{16}$$

The emergence of cell polarity relies on the (Turing) instability of the homogeneous steady state. To achieve that, two conditions are required:

- (i) If the perturbation is spatially homogeneous, the homogeneous steady state  $(a_0, b_0)$  is linearly stable. This condition ensures that starting from a constant initial condition close to  $(a_0, b_0)$ ,  $(a_0, b_0)$  will be an attractor. This condition is equivalent to that when the wave number  $k$  is zero, all eigenvalues  $\lambda$  are negative;
- (ii) For some positive integers  $k$ , at least one  $\lambda$  satisfying Eq. (16) is positive, which means that  $(a_0, b_0)$  is linearly unstable under a perturbation with some positive wave lengths (Turing 1990; Rätz and Röger 2012).

Together, these two conditions imply that wave functions perturbed from the homogeneous steady state are moving toward another steady state for and only for positive wave lengths.

The first condition is equivalent to that when  $k = 0$ , the trace of  $\mathbf{J}$  is negative and the determinant of  $\mathbf{J}$  is positive:

$$(F_{X_1} + na_0^{n-1}F_{X_2})b_0 - k_{\text{off}} - F - g_{\text{on}} - g_{\text{off}} < 0, \tag{17}$$

and

$$- (g_{\text{on}} + g_{\text{off}})((F_{X_1} + na_0^{n-1}F_{X_2})b_0 - k_{\text{off}}) + Fg_{\text{on}} > 0. \tag{18}$$

The inequality (18) can be rewritten as

$$(F_{X_1} + na_0^{n-1}F_{X_2})b_0 - k_{\text{off}} - \frac{g_{\text{on}}}{g_{\text{on}} + g_{\text{off}}}F < 0. \tag{19}$$

It is easy to show that (19) implies (17), and therefore one only needs to check the inequality (19) for condition (i).

The second condition is equivalent to the conditions that for some positive  $k$ , the determinant of  $\mathbf{J}$  is negative or the trace of  $\mathbf{J}$  is positive:

$$- 2\sigma_k D_m + F_{X_1}b_0 - k_{\text{off}} - F - g_{\text{off}} > 0 \tag{20}$$

or

$$\sigma_k^2 D_m^2 - \sigma_k D_m (F_{X_1}b_0 - k_{\text{off}} - F - g_{\text{off}}) - g_{\text{off}}(F_{X_1}b_0 - k_{\text{off}}) < 0, \quad k \geq 1. \tag{21}$$

As  $(a_0, b_0)$  is a homogeneous steady state, we can apply equality (8) to Eqs. (20) and (21), and rewrite them as

$$- 2\sigma_k D_m + \frac{g_{\text{on}}}{g_{\text{on}} + g_{\text{off}}}F_{X_1}(1 - a_0) - k_{\text{off}} - F - g_{\text{off}} > 0 \tag{22}$$

and

$$- \sigma_k D_m + \frac{g_{\text{on}}}{g_{\text{on}} + g_{\text{off}}}F_{X_1}(1 - a_0) - k_{\text{off}} - \frac{\sigma_k D_m}{\sigma_k D_m + g_{\text{off}}}F > 0. \tag{23}$$

It can be observed that the inequality (22) implies (23). Since (22) or (23) needs to be satisfied, it suffices to check the inequality (23).

Moreover, if there exists a positive integer  $k_c$  such that

$$-\sigma_{k_c} D_m + \frac{g_{\text{on}}}{g_{\text{on}} + g_{\text{off}}} F_{X_1} (1 - a_0) - k_{\text{off}} - \frac{\sigma_{k_c} D_m}{\sigma_{k_c} D_m + g_{\text{off}}} F > 0,$$

then the inequality (23) holds for any positive integer  $k \leq k_c$ . Thus, the second condition can be reduced to

$$-\sigma_1 D_m + \frac{g_{\text{on}}}{g_{\text{on}} + g_{\text{off}}} F_{X_1} (1 - a_0) - k_{\text{off}} - \frac{\sigma_1 D_m}{\sigma_1 D_m + g_{\text{off}}} F > 0. \quad (24)$$

Finally, we summarize that Turing instability exists at a homogeneous steady state solution  $(a_0, b_0)$  if the system (1)–(2) satisfies the following two conditions

$$\frac{g_{\text{on}}}{g_{\text{on}} + g_{\text{off}}} (F_{X_1} + n a_0^{n-1} F_{X_2}) (1 - a_0) - k_{\text{off}} - \frac{g_{\text{on}}}{g_{\text{on}} + g_{\text{off}}} F < 0, \quad (25)$$

and

$$-\sigma_1 D_m + \frac{g_{\text{on}}}{g_{\text{on}} + g_{\text{off}}} F_{X_1} (1 - a_0) - k_{\text{off}} - \frac{\sigma_1 D_m}{\sigma_1 D_m + g_{\text{off}}} F > 0. \quad (26)$$

When the conditions (25) and (26) are satisfied, positive  $\lambda_k$  can be solved from (16) for some positive  $k$ :

$$\lambda_k = \frac{-2\sigma_k + Q_1 + \sqrt{Q_1^2 + g_{\text{off}} Q_2}}{2}, \quad (27)$$

where  $Q_1 = \frac{g_{\text{on}}}{g_{\text{on}} + g_{\text{off}}} F_{X_1} (1 - a_0) - k_{\text{off}} - F - g_{\text{off}}$  and  $Q_2 = \frac{g_{\text{on}}}{g_{\text{on}} + g_{\text{off}}} F_{X_1} (1 - a_0) - k_{\text{off}}$ . We remark that  $Q_2$  is larger than zero since (26) is satisfied.

Since  $\sigma_k$  is increasing with respect to  $k \geq 1$ ,  $\lambda_k$  is decreasing with respect to  $k \geq 1$ . Then the fastest growing mode occurs when  $k = 1$ . This supports that single peak mode may dominate until reaching steady state and the model will end up with a single peak.

#### 4 Linear Feedback is Not Sufficient for Achieving Symmetry Breaking

The simplest form of feedback is a linear function dependent only on the density of the active polarized species  $a$ , namely,

$$F(a) = k_{11} + k_{12}a.$$

To see if this form of feedback can produce spontaneous cell polarization, one needs to check (25) and (26). Considering the term

$$\frac{g_{\text{on}}}{g_{\text{on}} + g_{\text{off}}} F_{X_1}(1 - a_0) - k_{\text{off}}$$

in (26), since  $a_0$  is a homogeneous steady state solution, by the equality (9), we deduce that

$$\begin{aligned} \frac{g_{\text{on}}}{g_{\text{on}} + g_{\text{off}}} F'(1 - a_0) - k_{\text{off}} &= \frac{1}{a_0} \left( \frac{g_{\text{on}}}{g_{\text{on}} + g_{\text{off}}} k_{12} a_0 (1 - a_0) - k_{\text{off}} a_0 \right) \\ &= - \frac{g_{\text{on}}}{g_{\text{on}} + g_{\text{off}}} \frac{k_{11} (1 - a_0)}{a_0} < 0. \end{aligned}$$

Therefore, the left-hand side of (26) is negative, and the second condition of Turing instability is not satisfied.

Although the above analysis suggests that linear positive feedback will not give rise to polarity establishment, this feedback was used in Altschuler et al. (2008) and was able to produce spontaneous polarization under a stochastic setting for budding yeast cells. This work (Altschuler et al. 2008) definitely has shown the effect of random fluctuation and demonstrated the essential difference between deterministic and stochastic models. However, while the feedback of Cdc42 cycle during yeast budding involves the recruitment of guanine nucleotide exchange factors, i.e., the GEF, and the formation of the Bem1 complexes including the GEF (Park and Bi 2007), the feedback is more likely a multi-step cooperative process than a linear one. Hence, we will consider the cooperative feedback in the following section.

### 5 Cooperative Feedback can Lead to Symmetry Breaking

A multiple-step cooperative feedback process can be modeled by a local feedback function with  $n \geq 2$ :

$$F(a) = k_{11} + k_{12} a^n, \quad n \geq 2, \tag{28}$$

where the parameter  $n$  determines the cooperativity of the response to the density of molecules. Here  $n = 1$  indicates a non-cooperative, while  $n > 1$  represents a multiple-step cooperative feedback process which may include different independent steps of recruitment, binding, and dissociation. In this section, we will show that our model coupling (28) can achieve Turing instability in some suitable parameter ranges.

Let  $(a_0, b_0)$  be a homogeneous steady state solution. According to (9),  $a_0$  satisfies the following equation

$$\frac{g_{\text{on}}}{g_{\text{on}} + g_{\text{off}}} (k_{11} + k_{12} a_0^n) (1 - a_0) - k_{\text{off}} a_0 = 0. \tag{29}$$

Defining  $k_3 = \frac{g_{\text{on}}}{g_{\text{on}} + g_{\text{off}}} k_{11}$  and  $k_4 = \frac{g_{\text{on}}}{g_{\text{on}} + g_{\text{off}}} k_{12}$ , we can rewrite (29) in a polynomial form

$$-k_4 a_0^{n+1} + k_4 a_0^n - (k_3 + k_{\text{off}}) a_0 + k_3 = 0. \tag{30}$$

Now we define the left-hand side as a function

$$f(a) = -k_4 a^{n+1} + k_4 a^n - (k_3 + k_{\text{off}})a + k_3. \tag{31}$$

According to the intermediate value theorem and the fact that  $f(0) > 0$  and  $f(1) < 0$ , at least one solution  $a_0$  of (30) exists between 0 and 1. Since  $f$  has only one inflection point  $a = \frac{n-1}{n+1}$  between 0 and 1, and there are at most three positive solutions satisfying (30) for  $n = 3$ , one can plot all the possible profiles of  $f$ , as shown in Fig. 2. We recall that  $(a_0, b_0)$  is locally stable for spatially homogeneous perturbations when it satisfies the inequality (25), which in this case can be rewritten as

$$(nk_4 a_0^{n-1})(1 - a_0) - k_{\text{off}} - (k_3 + k_4 a_0^n) < 0. \tag{32}$$

From (32), we know that (25) is satisfied if and only if the slope of  $f$  is negative at  $a = a_0$ .

If  $f$  assumes one of the profiles in Fig. 2a–e, there is always at least one homogeneous steady state solution satisfying condition (25). If  $f$  is a function as in Fig. 2f, the slope of  $f$  is zero at  $a = a_0$ ; however, by considering higher order terms, it is easy to show that the homogeneous steady state is locally stable for spatially homogeneous perturbations. Hence, we can conclude that there always exists at least one homogeneous steady state solution which is locally stable for spatially homogeneous perturbations.

To obtain Turing instability, besides satisfying (25), a homogeneous steady state solution has to be unstable for a perturbation with some positive wavenumbers  $k$ , that is, to satisfy (26). The following theorem provides a range of parameters in which Turing instability exists, and later another theorem will be stated, which gives a condition for the existence of locally stable homogeneous steady state solution. In the following theorem, we define  $D^* = \sigma_1 D_m + \frac{\sigma_1 D_m}{\sigma_1 D_m + g_{\text{off}}}(k_{11} + k_{12})$ . The detailed proofs are presented in Appendix 7.2.

**Theorem 1** Assume that  $D^* < k_3$  and  $n > 1$ . For the system (1)–(2) with the local feedback form (28), if the condition

$$1 - \frac{(n-1) \frac{n-1}{n} k_{\text{off}} + D^*}{n \frac{1}{k_4^n} k_3^n} > \frac{k_3}{k_3 - \frac{1}{n} D^* + \frac{n-1}{n} k_{\text{off}}} \tag{33}$$

is satisfied, then there exists a homogeneous steady state solution satisfying conditions (25) and (26) for Turing instability. In addition, the condition (33) also implies that there is no locally stable homogeneous steady state solution.

By Theorem 1, we find that Turing instability can be obtained with suitable ranges of parameters. Now we use a computational simulation for one-dimensional model to verify the result of Theorem 1. For the simulations in this paper, we apply a second-order central difference approximation for the diffusion terms, Riemann sum for the definite integrals, and a fourth order Adams–Moulton predictor–corrector method for

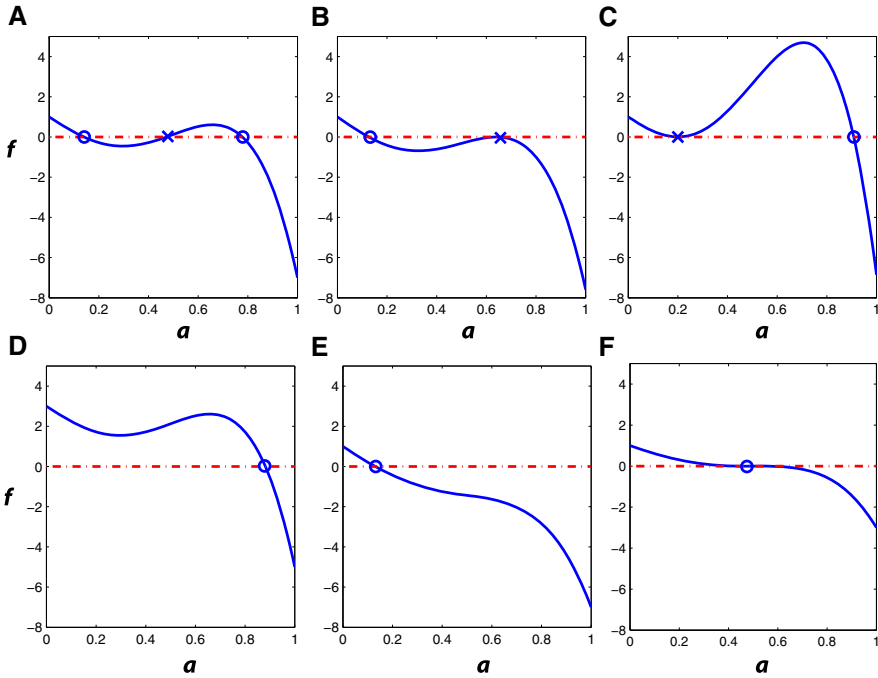


**Fig. 2** Possible combinations of homogeneous steady states of model (1)–(2), with feedback form (28) and  $n \geq 2$ . Circle markers represent homogeneous steady states which are locally stable for spatially homogeneous perturbation; cross markers represent homogeneous steady states which are locally unstable for spatially homogeneous perturbation. In all the plots, we take  $n = 3$  with parameters: **a**  $k_3 = 1 \text{ min}^{-1}$ ,  $k_4 = 50 \text{ min}^{-1}$ , and  $k_{\text{off}} = 7 \text{ min}^{-1}$ ; **b**  $k_3 = 1 \text{ min}^{-1}$ ,  $k_4 = 47.6837 \text{ min}^{-1}$ , and  $k_{\text{off}} = 7.5938 \text{ min}^{-1}$ ; **c**  $k_3 = 1 \text{ min}^{-1}$ ,  $k_4 = 89.2857 \text{ min}^{-1}$ , and  $k_{\text{off}} = 6.8571 \text{ min}^{-1}$ ; **d**  $k_3 = 3 \text{ min}^{-1}$ ,  $k_4 = 50 \text{ min}^{-1}$ , and  $k_{\text{off}} = 3 \text{ min}^{-1}$ ; **e**  $k_3 = 1 \text{ min}^{-1}$ ,  $k_4 = 25 \text{ min}^{-1}$ , and  $k_{\text{off}} = 7 \text{ min}^{-1}$ ; **f**  $k_3 = 1 \text{ min}^{-1}$ ,  $k_4 = 16 \text{ min}^{-1}$ , and  $k_{\text{off}} = 3 \text{ min}^{-1}$

the temporal discretization. FORTRAN 77 is used for the simulation and plots are generated using MATLAB. For one-dimensional simulations, the number of spatial points is 400 and the temporal step  $\Delta t$  is  $1 \times 10^{-3} \text{ min}$ ; for two-dimensional simulations, the number of spatial points is 1,026 and the temporal step  $\Delta t$  is  $6.64 \times 10^{-4} \text{ min}$ . The initial conditions for all simulations are defined as

$$\begin{aligned}
 a(x, 0) &= 0, \\
 b(x, 0) &= 0.3(1 + 0.2\eta(x)),
 \end{aligned}$$

where  $\eta(x)$  is a function of uniformly distributed random number from 0 to 1.

The time-dependent simulation shown in Fig. 3a demonstrates that localization of active signaling molecules can be achieved with a set of parameters satisfying (33). The ranges of the parameters we use here are based on previous works (Lo et al. 2013; Goryachev and Pokhilko 2008; Altschuler et al. 2008).

We are also interested in the range of parameters in which a solution may tend to a homogeneous steady state, as stated in the following theorem.

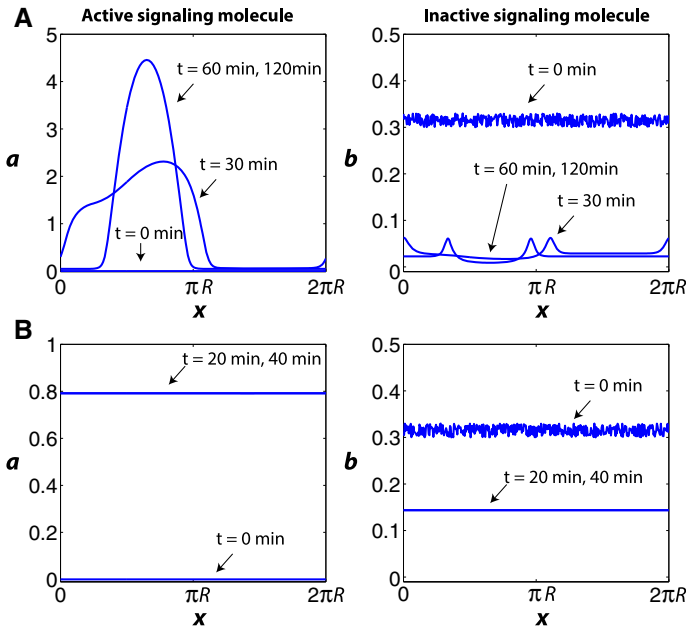


**Fig. 3** Time-dependent simulations for the one-dimensional model (1)–(2) with the local feedback (28). *Left panels* are solutions of *a* and *right panels* are solutions of *b*. In these two simulations,  $n = 2$ ,  $D = 0.15 \mu\text{m}^2 \text{min}^{-1}$ ,  $R = 2 \mu\text{m}$ ,  $k_{\text{off}} = 10 \text{min}^{-1}$ ,  $g_{\text{on}} = 20 \text{min}^{-1}$ , and  $g_{\text{off}} = 9 \text{min}^{-1}$ . Other parameters are: **a**  $k_{11} = 20 \text{min}^{-1}$  and  $k_{12} = 250 \text{min}^{-1}$ ; **b**  $k_{11} = 30 \text{min}^{-1}$  and  $k_{12} = 40 \text{min}^{-1}$

**Theorem 2** Assume that  $n > 1$ . For the system (1)–(2) with the local feedback form (28), if the condition

$$1 - \frac{(n-1)^{\frac{n-1}{n}} k_{\text{off}}}{n k_4^{\frac{1}{n}} k_3^{\frac{n-1}{n}}} < \frac{k_3}{k_3 + \frac{n-1}{n} k_{\text{off}}} \quad (34)$$

is satisfied, then there exists a locally stable homogeneous steady state solution. This means that an evolving solution may stabilize to a homogeneous steady state when the initial condition is sufficiently close to it.

The simulation displayed in Fig. 3b demonstrates that if the parameters satisfy the inequality (34), the solution tends to a homogeneous steady state.

As mentioned above, the feedback loop on activation of signaling molecules usually is a multiple step process involving recruitment and binding of certain feedback molecules, such as Bem1 complex and Rdi1 protein. A growing Cdc42-GTP cluster on the cell membrane captures free feedback molecules in the cytoplasm and then, the membrane-bound feedback molecules promote and maintain the local clustering of active Cdc42. The limitation of the total amount of feedback molecules implies that the magnitude of feedback saturates; however, this saturation is not modeled in the current feedback form (28). Motivated by this, we study a non-local feedback function in the next section.

### 6 Non-local Feedback Enhances Sharper and Faster Polarization

If we take into account the molecules which mediate the positive feedback (here we call them feedback molecules), as shown in Fig. 1b, and assume that these molecules are initially uniformly distributed in the cytoplasm and later recruited to the cell membrane by the active signaling molecules (variable  $a$ ), then the activation rate of the signaling molecules is proportional to the density of the membrane-bound feedback molecules (denoted by  $c$ ). Thus, we obtain the following equations for  $a$ ,  $b$ , and  $c$ :

$$\frac{\partial a}{\partial t} = D_m \nabla^2 a + k_{on}cb - k_{off}a, \tag{35}$$

$$\frac{\partial b}{\partial t} = D_m \nabla^2 b - k_{on}cb + k_{off}a + g_{on}(1 - \hat{a} - \hat{b}) - g_{off}b, \tag{36}$$

$$\frac{\partial c}{\partial t} = (h_1 + h_2a^n)(1 - \hat{c}) - h_{off}c, \tag{37}$$

where  $(h_1 + h_2a^n)$  is the recruitment rate of the feedback molecules  $c$  from the cytoplasm to the membrane, the parameter  $h_1$  is the basal recruitment rate of the feedback molecules and he parameter  $h_2$  is the Cdc42-mediated recruitment rate of the feedback molecules;  $(1 - \hat{c})$  is the fraction of the cytoplasmic feedback molecules;  $\hat{c}$  represents the average value of  $c$  over the membrane; and  $h_{off}$  is the disassociation rate of the feedback molecules from the membrane to the cytoplasm.

We assume that the dynamics of the feedback molecules is much faster than that of the signaling molecules, as in Goryachev and Pokhilko (2008), Lo et al. (2013). Therefore, particle density of the feedback molecules reaches quasi-steady state of Eq. (37) at the time scale of  $a$  and  $b$ , that is,

$$(h_1 + h_2a^n)(1 - \hat{c}) - h_{off}c = 0.$$

By integrating the above equation over the membrane, one can obtain the value of  $\hat{c}$  and substitute that back into the equation, and then we have

$$c = \frac{k_{21} + k_{22}a^n}{1 + k_{21} + k_{22}\hat{a}^n}, \tag{38}$$

where  $k_{21}$  and  $k_{22}$  equal to  $h_1/h_{off}$  and  $h_2/h_{off}$ , respectively.

By substituting (38) into Eqs. (35) and (36), we obtain a system with a non-local feedback term:

$$\begin{aligned} \frac{\partial a}{\partial t} &= D_m \nabla^2 a + F(a, \hat{a}^n)b - k_{off}a, \\ \frac{\partial b}{\partial t} &= D_m \nabla^2 b - F(a, \hat{a}^n)b + k_{off}a + g_{on}(1 - \hat{a} - \hat{b}) - g_{off}b, \end{aligned}$$

with

$$F(a, \hat{a}^n) = k_{on} \frac{k_{21} + k_{22}a^n}{1 + k_{21} + k_{22}\hat{a}^n}. \tag{39}$$

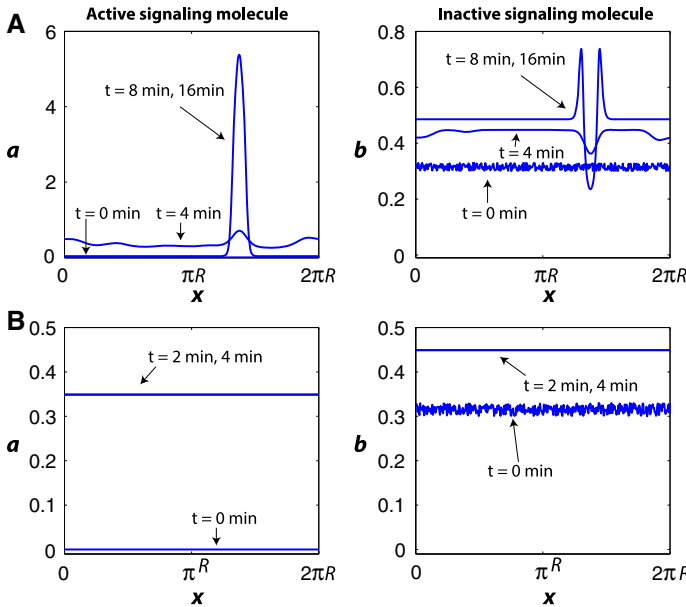


**Fig. 4** Time-dependent simulations for the one-dimensional model (1)–(2) with the non-local feedback (39). *Left panels* are solutions of *a* and *right panels* are solutions of *b*. In these two simulations,  $n = 2$ ,  $D = 0.15 \mu\text{m}^2 \text{min}^{-1}$ ,  $R = 2 \mu\text{m}$ ,  $k_{\text{on}} = 10 \text{min}^{-1}$ ,  $k_{\text{off}} = 10 \text{min}^{-1}$ ,  $g_{\text{on}} = 20 \text{min}^{-1}$ , and  $g_{\text{off}} = 9 \text{min}^{-1}$ . Other parameters are: **a**  $k_{21} = 2$  and  $k_{22} = 25$ ; **b**  $k_{21} = 3$  and  $k_{22} = 4$

Hence, the three-equation system is reduced to a two-equation system, but with the positive feedback as a non-local function of *a*, unlike the usual feedback forms.

Now we study the parameter regime for achieving symmetry breaking. First, we start our analysis by considering the steady state equation (9)

$$\frac{k_5 + k_6 a_0^n}{1 + k_1 + k_2 a_0^n} (1 - a_0) - k_{\text{off}} a_0 = 0. \tag{40}$$

By denoting  $k_{\text{on}}^* = \frac{g_{\text{on}}}{g_{\text{on}} + g_{\text{off}}} k_{\text{on}}$ ,  $k_5 = k_{\text{on}}^* k_{21}$ , and  $k_6 = k_{\text{on}}^* k_{22}$ , Eq. (40) can be rewritten as

$$\frac{1}{1 + k_{21} + k_{22} a_0^n} \left( (k_5 + k_6 a_0^n) \left( 1 - \frac{k_{\text{on}}^* + k_{\text{off}}}{k_{\text{on}}^*} a_0 \right) - k_{\text{off}} a_0 \right) = 0. \tag{41}$$

Let the left-hand side be a function  $g(a)$ :

$$g(a) = \frac{1}{1 + k_{21} + k_{22} a^n} g_1(a),$$

where

$$g_1(a) = (k_5 + k_6 a^n) \left( 1 - \frac{k_{\text{on}}^* + k_{\text{off}}}{k_{\text{on}}^*} a \right) - k_{\text{off}} a. \tag{42}$$

It is easy to see that  $g(a) = 0$  if and only if  $g_1(a) = 0$ . Moreover, for any  $a_0$  satisfying  $g(a_0) = 0$  (or equivalently  $g_1(a_0) = 0$ ), we have  $g'_1(a_0) < 0$  if and only



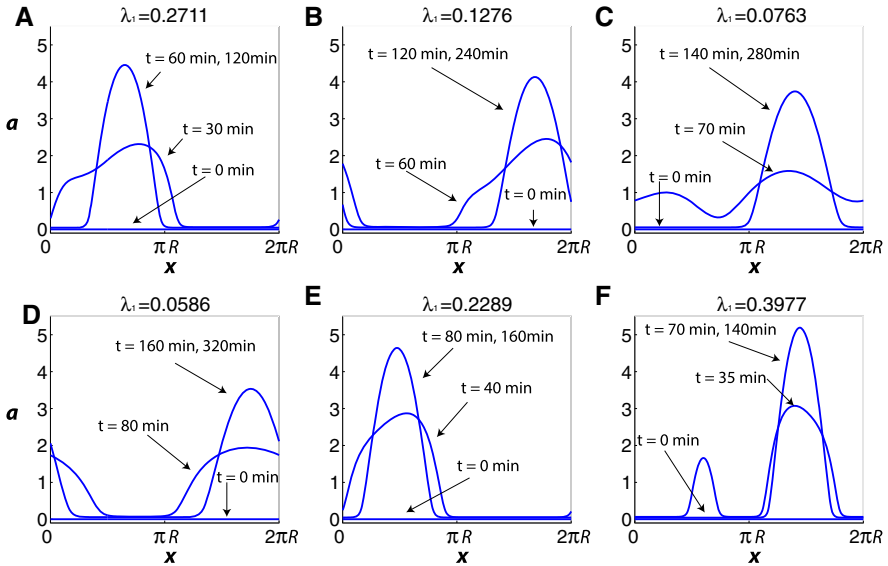


**Fig. 5** Time-dependent solutions of  $a$  for the one-dimensional model (1)–(2) with the local feedback (28). In all these simulations,  $n = 2$ ,  $D = 0.15 \mu\text{m}^2 \text{min}^{-1}$ ,  $R = 2 \mu\text{m}$ ,  $g_{\text{on}} = 20 \text{min}^{-1}$ , and  $g_{\text{off}} = 9 \text{min}^{-1}$ . Other parameters are: **a**  $k_{11} = 20 \text{min}^{-1}$ ,  $k_{12} = 250 \text{min}^{-1}$  and  $k_{\text{off}} = 10 \text{min}^{-1}$ ; **b**  $k_{11} = 36 \text{min}^{-1}$ ,  $k_{12} = 450 \text{min}^{-1}$ , and  $k_{\text{off}} = 10 \text{min}^{-1}$ ; **c**  $k_{11} = 50 \text{min}^{-1}$ ,  $k_{12} = 650 \text{min}^{-1}$ , and  $k_{\text{off}} = 10 \text{min}^{-1}$ ; **d**  $k_{11} = 30 \text{min}^{-1}$ ,  $k_{12} = 375 \text{min}^{-1}$ , and  $k_{\text{off}} = 5 \text{min}^{-1}$ ; **e**  $k_{11} = 30 \text{min}^{-1}$ ,  $k_{12} = 375 \text{min}^{-1}$ , and  $k_{\text{off}} = 13 \text{min}^{-1}$ ; **f**  $k_{11} = 30 \text{min}^{-1}$ ,  $k_{12} = 375 \text{min}^{-1}$  and  $k_{\text{off}} = 20 \text{min}^{-1}$

if  $g'(a_0) < 0$ . Thus, the stability analysis reduces to analysis based on  $g_1$ . Note that the function form of  $g_1$  in Eq. (42) is similar to the polynomial form feedback  $f$  in Eq. (31), so the stability analysis for spatially homogeneous perturbations we did in Sect. 5 can be carried out similarly here. After applying the result in Sect. 5, we conclude that at least one homogeneous steady state solution is locally stable for spatially homogeneous perturbations in the system (1)–(2) with the feedback form (39).

Next we want to find a range of parameter in which a steady state solution is unstable for a perturbation with certain positive wavenumbers  $k$  (satisfying (26)) for obtaining Turing instability. In the following theorem, we define  $D^+ = \sigma_1 D_m + \frac{\sigma_1 D_m}{\sigma_1 D_m + g_{\text{off}}} \frac{k_{21} + k_{22}}{1 + k_{21} + k_{22}}$ . The proof of the following theorem can be found in Appendix 7.2.

**Theorem 3** Assume that  $D^+ < k_5$  and  $n > 1$ . For the system (1)–(2) with the non-local feedback form (39), if the condition

$$1 - \frac{(n-1) \frac{n-1}{n} k_{\text{off}} + D^+}{n \frac{1}{k_6^n k_5^n}} > \frac{k_5}{k_5 - \frac{1}{n} \frac{k_{\text{on}}^*}{k_{\text{on}}^* + k_{\text{off}}} D^+ + \frac{n-1}{n} \frac{k_{\text{on}}^*}{k_{\text{on}}^* + k_{\text{off}}} k_{\text{off}}} \tag{43}$$

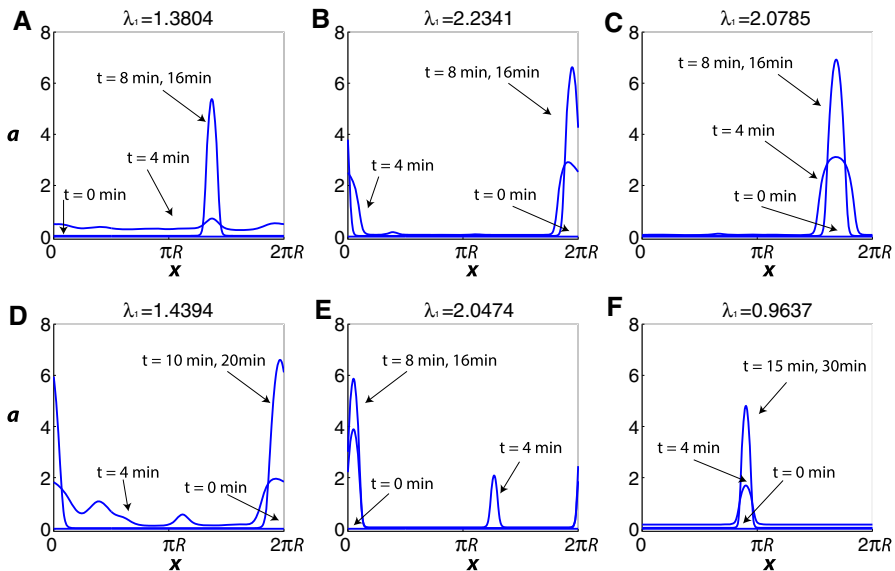


**Fig. 6** Time-dependent solutions of  $a$  for the one-dimensional model (1)–(2) with the non-local feedback (39). In all these simulations,  $n = 2$ ,  $D = 0.15 \mu\text{m}^2 \text{min}^{-1}$ ,  $R = 2 \mu\text{m}$ ,  $k_{21} = 2$ ,  $k_{22} = 25$ ,  $g_{\text{on}} = 20 \text{min}^{-1}$ , and  $g_{\text{off}} = 9 \text{min}^{-1}$ . Other parameters are: **a**  $k_{\text{on}} = 10 \text{min}^{-1}$  and  $k_{\text{off}} = 10 \text{min}^{-1}$ ; **b**  $k_{\text{on}} = 18 \text{min}^{-1}$  and  $k_{\text{off}} = 10 \text{min}^{-1}$ ; **c**  $k_{\text{on}} = 25 \text{min}^{-1}$  and  $k_{\text{off}} = 10 \text{min}^{-1}$ ; **d**  $k_{\text{on}} = 15 \text{min}^{-1}$  and  $k_{\text{off}} = 5 \text{min}^{-1}$ ; **e**  $k_{\text{on}} = 15 \text{min}^{-1}$  and  $k_{\text{off}} = 13 \text{min}^{-1}$ ; **f**  $k_{\text{on}} = 15 \text{min}^{-1}$  and  $k_{\text{off}} = 18 \text{min}^{-1}$

is satisfied, then there exists a homogeneous steady state solution satisfying conditions (25) and (26) for Turing instability. In addition, condition (43) also implies that a locally stable homogeneous steady state solution does not exist.

The time-dependent simulation shown in Fig. 4a demonstrates that one set of parameter that satisfies the condition (43) gives rise to localization of signaling molecules for the one-dimensional model.

In the next theorem, we provide conditions for which the homogeneous steady state is locally stable. The proof of the following theorem can be found in Appendix 7.2.

**Theorem 4** Assume that  $n > 1$ . For the system (1)–(2) with the non-local feedback form (39), if the condition

$$1 - \frac{(n-1) \frac{n-1}{n} k_{\text{off}}}{n k_6^n k_5^{\frac{n-1}{n}}} < \frac{k_5}{k_5 + \frac{n-1}{n} \frac{k_{\text{on}}^*}{k_{\text{on}}^* + k_{\text{off}}} k_{\text{off}}} \tag{44}$$

is satisfied, then there exists a locally stable homogeneous steady state solution.

In Fig. 4b, we choose one set of parameters that satisfies the the inequality (44), and run a simulation. The solution indeed approaches a homogeneous steady state.

Comparing the simulations in Figs. 3 and 4, we observe that with the non-local feedback (39), the polarization is sharper and forms faster than that with the local feedback (28). To test if this is a general trend, we vary the activation rate and deactivation rate coefficients, while keeping the diffusion rate  $D_m$ , the recruitment rate  $g_{\text{on}}$

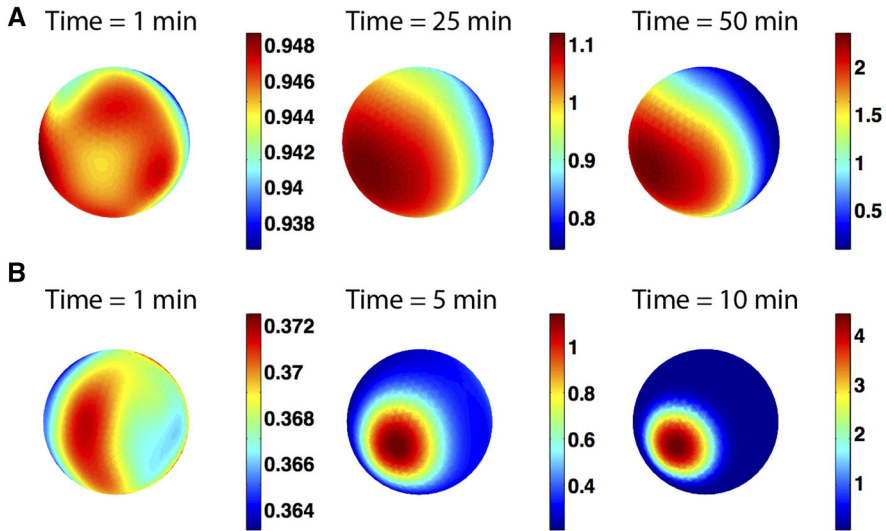


**Fig. 7** (Color Figure Online) Time-dependent solutions of  $a$  for the two-dimensional model (1)–(2). **a** With the local feedback (28). In this simulation,  $n = 2$ ,  $D = 0.15 \mu\text{m}^2 \text{min}^{-1}$ ,  $R = 2 \mu\text{m}$ ,  $g_{\text{on}} = 20 \text{min}^{-1}$ ,  $g_{\text{off}} = 9 \text{min}^{-1}$ ,  $k_{11} = 20 \text{min}^{-1}$ ,  $k_{12} = 250 \text{min}^{-1}$ , and  $k_{\text{off}} = 10 \text{min}^{-1}$ ; **b** with the non-local feedback (39). In this simulation,  $n = 2$ ,  $D = 0.15 \mu\text{m}^2 \text{min}^{-1}$ ,  $R = 2 \mu\text{m}$ ,  $k_{21} = 2$ ,  $k_{22} = 25$ ,  $g_{\text{on}} = 20 \text{min}^{-1}$ ,  $g_{\text{off}} = 9 \text{min}^{-1}$ ,  $k_{\text{on}} = 10 \text{min}^{-1}$ , and  $k_{\text{off}} = 10 \text{min}^{-1}$

and the extraction rate  $g_{\text{off}}$  fixed, with their values based on Altschuler et al. (2008), Lo et al. (2013). Figure 5 shows that with the local feedback (28), the polarization always reaches steady state after 60 min. On the other hand, the system with the non-local feedback (39) produces a sharper polarization and the polarity is stabilized around 10 min (Fig. 6). If we compare the growth rates,  $\lambda_1$ , of the fastest growing mode, we find that  $\lambda_1$  for the non-local feedback (39), which is between 0.9 and 2.3, is much larger than that for the local feedback (28), which is between 0.05 and 0.4. This result supports that the non-local feedback (39) enables faster polarization. In yeast budding, the localization of membrane-bound Cdc42-GTP is usually very sharp and forms rapidly, usually in not more than 60 min. We also compare the simulations of the two feedback functions for the two-dimensional model and the results are consistent with that observed in the one-dimensional simulations. Figure 7 displays two examples of the simulations for the two feedback functions on the two-dimensional spherical surface. With the local feedback (28), the polarization reaches steady state after 50 min (Fig. 7a); the system with the non-local feedback (39) produces a sharper polarization within 10 min (Fig. 7b). Our simulations suggest that, the non-local feedback (39) may play a positive role in the formation of a narrow polarization and fast dynamics, with diffusion and recruitment rates within some reasonable ranges.

### 7 Conclusion

Mathematical modeling is an important tool to understand the mechanisms of cell polarity establishment and maintenance. Numerous models have been proposed for

different systems of cell polarization (Altschuler et al. 2008; Goryachev and Pokhilko 2008; Jilkinе and Edelstein-Keshet 2011; Rätz and Röger 2012). For budding yeast system, recent studies suggest that spontaneous emergence can be achieved through cycling of active and inactive Cdc42 molecules and the positive feedback through Bem1 complex (Altschuler et al. 2008; Goryachev and Pokhilko 2008) or Rdi1 protein (Smith et al. 2013). However, detailed mathematical analysis of the models is not well studied in this system.

In this paper, we have formulated a two-equation model of reaction-diffusion systems for cell polarization, which encompasses many previous polarization models for yeast and other organisms. Our model consists of active and inactive forms of the polarization molecules, and involves a general form of positive feedback, which could be local or non-local. We have used Turing stability analysis to analyze the conditions and the forms of feedbacks that can give rise to spontaneous cell polarization. It is shown in this paper that linear positive feedback is not sufficient to achieve cell polarization, while cooperative feedback or non-local feedback due to mediating feedback molecules are good for polarization. Moreover, our results reveal that the diffusion rates of active and inactive signaling molecules do not need to be very different in order to produce cell polarization. Finally, our simulations suggest that the molecule-mediated feedback, which corresponds to the non-local feedback form, plays a positive role in narrowing the localization area as well as fast dynamics to achieve robust polarization. The conclusions in this paper provide parameter conditions that can be checked for the existence of polarized solutions. Furthermore, the analysis of the feedback provides insights into the mechanisms through which cell polarity is established.

In this study, we only focus on spontaneous emergence of cell polarization which do not involve inherited spatial cues, such as the budding landmark cues in the normal budding of yeast cells. Previous studies have shown that cells also exhibit a characteristic and robust pattern of polarization dependent on specific type of spatial cues (Jilkinе and Edelstein-Keshet 2011; Lo et al. 2013; Moore et al. 2008; Park and Bi 2007). In the future work, we will extend our study to these systems [for example, a yeast model with landmark cues in Lo et al. (2013)] to get better insights into these biological processes.

**Acknowledgments** This research has been supported by the Mathematical Biosciences Institute and the National Science Foundation under Grant DMS 0931642. Ching-Shan Chou is supported by National Science Foundation under Grant DMS 1020625 and DMS 1253481.

## Appendix

### 7.1 Proofs of Lemmas

In this section, we will state three lemmas, which will be used in the next section for the proofs of Theorems 1–4. First, we define a function  $f_y(a)$  used in the lemmas:

$$f_y(a) = (\gamma_1 + \gamma_2 a^n)(1 - \gamma_3 y) - \gamma_4 a - D(a - y). \quad (45)$$

where  $n > 1$ ,  $\gamma_1, \gamma_2, \gamma_4 > 0$ ,  $\gamma_3 \geq 1$  and  $0 \leq D < \gamma_1 \gamma_3$ .

**Lemma 1** *The function  $f_y$  in (45) has the following properties:*

1.  $\min_{a \geq 0} f_y(a)$  equals to

$$\gamma_1 - (\gamma_1\gamma_3 - D)y - \frac{n-1}{n^{n-1}} \frac{(\gamma_4 + D)^{\frac{n}{n-1}}}{\gamma_2^{\frac{1}{n-1}}} (1 - \gamma_3y)^{-\frac{1}{n-1}},$$

which is strictly decreasing with respect to  $y$  for  $y \in (0, 1/\gamma_3)$ .

2. For each  $y$ , there exist at most two solutions in  $\{a|a \geq 0\}$  satisfying  $f_y(a) = 0$ .
3. There exists a number  $y_m$  in  $[0, 1/\gamma_3)$  such that two smooth functions  $a_1(y), a_2(y)$  can be well defined in the domain  $[y_m, 1/\gamma_3)$  and the following properties hold:
  - (a)  $\min_{a \geq 0} f_y(a) \leq 0$  for any  $y \in [y_m, 1/\gamma_3)$ ;
  - (b)  $f_y(a_1(y)) = f_y(a_2(y)) = 0$  for any  $y \in [y_m, 1/\gamma_3)$ ;
  - (c)  $a_1(y) > a_2(y) \geq 0$  for any  $y \in (y_m, 1/\gamma_3)$ ;
  - (d)  $a'_1(y) > 0$  and  $a'_2(y) < 0$  for any  $y \in (y_m, 1/\gamma_3)$ ;
  - (e)  $\lim_{y \rightarrow 1/\gamma_3} a_1(y) = \infty$  and  $\lim_{y \rightarrow 1/\gamma_3} a_2(y) = 0$ ;
  - (f)  $\frac{df_y}{da} \Big|_{a=a_1(y)} > 0$  and  $\frac{df_y}{da} \Big|_{a=a_2(y)} < 0$  for any  $y \in (y_m, 1/\gamma_3)$ ;
  - (g) if there is at least one solution in  $a \geq 0$  for  $f_0(a) = 0$ , then  $y_m = 0$ ;
  - (h) if there is no solution in  $a \geq 0$  for  $f_0(a) = 0$ , then  $a_1(y_m) = a_2(y_m)$ ,  $\frac{df_{y_m}}{da} \Big|_{a=a_1(y_m)} = \frac{df_{y_m}}{da} \Big|_{a=a_2(y_m)} = 0$  and  $\min_{a \geq 0} f_{y_m}(a) = 0$ .

*Proof* 1. First we consider the first and second derivatives of  $f_y$ ,

$$\frac{df_y(a)}{da} = n\gamma_2 a^{n-1} (1 - \gamma_3y) - \gamma_4 - D, \tag{46}$$

$$\frac{d^2 f_y(a)}{da^2} = n(n-1)\gamma_2 a^{n-2} (1 - \gamma_3y). \tag{47}$$

By Eq. (47), we show that the minimum point in  $\{a|a \geq 0\}$ , with  $y \in (0, 1/\gamma_3)$ , is at

$$a = \left( \frac{\gamma_4 + D}{n\gamma_2(1 - \gamma_3y)} \right)^{\frac{1}{n-1}}$$

with

$$\min_{a \geq 0} f_y(a) = \gamma_1 - (\gamma_1\gamma_3 - D)y - \frac{n-1}{n^{n-1}} \frac{(\gamma_4 + D)^{\frac{n}{n-1}}}{\gamma_2^{\frac{1}{n-1}}} (1 - \gamma_3y)^{-\frac{1}{n-1}}.$$

By the given condition  $D < \gamma_1\gamma_3$ , it is easy to show that  $\min_{a \geq 0} f_y(a)$  is strictly decreasing with respect to  $y$ .

2. Suppose that  $y$  is a fixed number. If  $\min_{a \geq 0} f_y(a) > 0$ , there is no solution  $a \geq 0$  satisfying  $f_y(a) = 0$ .

If  $\min_{a \geq 0} f_y(a) = 0$ , the minimum point

$$\bar{a} = \left( \frac{\gamma_4 + D}{n\gamma_2(1 - \gamma_3 y)} \right)^{\frac{1}{n-1}}$$

is one of the roots for  $f_y(a)$ . As  $\frac{df_y(a)}{da} > 0$  for  $a > \bar{a}$  and  $\frac{df_y(a)}{da} < 0$  for  $0 \leq a < \bar{a}$ ,  $f_y(a) > f_y(\bar{a})$  for any  $a \neq \bar{a}$ , and therefore  $\bar{a}$  is the only solution of  $f_y(a) = 0$ .

If  $\min_{a \geq 0} f_y(a) < 0$ , by the fact that  $f_y(0) > 0$ ,  $\lim_{a \rightarrow \infty} f_y(a) > 0$  and the intermediate value theorem, we know that there are at least two solutions satisfying  $f_y(a) = 0$ . As  $\frac{df_y(a)}{da} > 0$  for  $a > \bar{a}$  and  $\frac{df_y(a)}{da} < 0$  for  $0 \leq a < \bar{a}$ ,  $f_y(a) > f_y(\bar{a})$  for any  $a \neq \bar{a}$ . So there are only two roots of  $f_y(a)$ : one is in  $[0, \bar{a})$ , and the other is in  $(\bar{a}, \infty)$ .

3. By the result of part 1,  $\min_{a \geq 0} f_y(a)$  tends to  $-\infty$  as  $y$  is close to  $1/\gamma_3$ . If  $\min_{a \geq 0} f_y(a) > 0$  for  $y = 0$ , according to the intermediate value theorem, we can find  $y_m$  such that  $\min_{a \geq 0} f_{y_m}(a)$  equals zero; if  $\min_{a \geq 0} f_y(a) \leq 0$  for  $y = 0$ , we define  $y_m = 0$ .

Since  $\min_{a \geq 0} f_y(a)$  is strictly decreasing with respect to  $y$ , and according to the results of part 2,  $f_y(a) = 0$  has two solutions  $a$  for any  $y \in (y_m, 1/\gamma_3)$ , so we can define two functions  $a_1(y)$  and  $a_2(y)$  that satisfy  $f_y(a_1(y)) = f_y(a_2(y)) = 0$  and  $a_1(y) > a_2(y)$  for any  $y \in (y_m, 1/\gamma_3)$ , that is,

$$a_1(y) = \max\{a \geq 0 | f_y(a) = 0\}, \quad a_2(y) = \min\{a \geq 0 | f_y(a) = 0\}.$$

The derivative of  $f_y(a)$  with respect to  $y$  is  $-\gamma_1\gamma_3 + D - \gamma_2\gamma_3a^n$ , which is always negative, and  $f_y(a)$  is a smooth function with respect to  $y$  and  $a$ , and therefore we can apply the inverse function theorem to show that  $a_1(y)$  and  $a_2(y)$  are smooth functions. By the definitions and the proof of part 2, it is easy to verify the properties (a, b, c, f, g, h).

By property (b), we have  $f_y(a_1(y)) = 0$  and  $f_y(a_2(y)) = 0$ . When differentiating these two equations with respect to  $y$  on both sides, we have  $-\gamma_1\gamma_3 + D - \gamma_2\gamma_3a_1(y)^n + \frac{df_y}{da}(a_1(y))a'_1(y) = 0$  and  $-\gamma_1\gamma_3 + D - \gamma_2\gamma_3a_2(y)^n + \frac{df_y}{da}(a_2(y))a'_2(y) = 0$ . Hence we obtain

$$a'_1(y) = -\frac{-\gamma_1\gamma_3 + D - \gamma_2\gamma_3a_1(y)^n}{\frac{df_y}{da}(a_1(y))},$$

$$a'_2(y) = -\frac{-\gamma_1\gamma_3 + D - \gamma_2\gamma_3a_2(y)^n}{\frac{df_y}{da}(a_2(y))}.$$

By property (f) and  $\gamma_1\gamma_3 > D$ , we show that  $a'_1(y) > 0$  and  $a'_2(y) < 0$ , which completes the proof of property (d).

From the proof of part 2, we have  $a_2 \in \left[ 0, \left( \frac{\gamma_4 + D}{n\gamma_2(1 - \gamma_3 y)} \right)^{\frac{1}{n-1}} \right)$  and  $a_1 \in \left( \left( \frac{\gamma_4 + D}{n\gamma_2(1 - \gamma_3 y)} \right)^{\frac{1}{n-1}}, \infty \right)$ . So we know that  $a_1(y)$  tends to infinity as  $y$  goes to  $1/\gamma_3$ .

Since  $a = 0$  is the solution for  $f_{1/\gamma_3}(a) = 0$ , we have  $\lim_{y \rightarrow 1/\gamma_3} a_2(y) = 0$ , which completes the proof of property (e). □

**Lemma 2** *If*

$$\left( 1 - \frac{(n-1)^{\frac{n-1}{n}}}{n} \frac{\gamma_4 + D}{\gamma_2^{\frac{1}{n}} \gamma_1^{\frac{n-1}{n}}} \right) > \frac{\gamma_1 \gamma_3}{\gamma_1 \gamma_3 - \frac{1}{n} D + \frac{n-1}{n} \gamma_4} \tag{48}$$

*is satisfied, then  $\frac{df_{a_0}}{da} \Big|_{a=a_0} > 0$  holds for any solution  $a_0$  satisfying  $f_{a_0}(a_0) = 0$ .*

For the proofs of Lemmas 2 and 3, we define two functions  $S_1, S_2$  in the domain  $[y_m, 1/\gamma_3)$ :

$$\begin{aligned} S_1(y) &= a_1(y) - y, \\ S_2(y) &= a_2(y) - y, \end{aligned}$$

where  $a_1, a_2$  and  $y_m$  are defined in Lemma 1.

*Proof* There are two parts in the proof:

1. Prove that if  $S_1(y_m) < 0$ ,  $\frac{df_{a_0}}{da} \Big|_{a=a_0} > 0$  holds for any solution  $a_0 \geq 0$  satisfying  $f_{a_0}(a_0) = 0$ .
2. Prove that condition (48) implies  $S_1(y_m) < 0$ .

By combining these two results, we can prove that if the condition (48) is satisfied, then  $\frac{df_{a_0}}{da} \Big|_{a=a_0} > 0$  holds for any solution  $a_0 \geq 0$  satisfying  $f_{a_0}(a_0) = 0$ . □

*Proof of part 1* Suppose that  $S_1(y_m) < 0$ . Since  $a_1(y) \geq a_2(y)$ , we get  $S_2(y_m) \leq S_1(y_m) < 0$ . By  $a'_2(y) < 0$  (Lemma 1(3c)), we have  $S'_2 < 0$ , which means that  $S_2$  is a decreasing function. Since  $S_2(y_m) < 0$  and  $S_2$  is a decreasing function,  $S_2(y) < 0$  for all  $y \in [y_m, 1/\gamma_3)$ , and there is no solution to  $S_2(y) = 0$ .

According to Lemma 1 and the definitions of  $S_1$  and  $S_2$ , all solutions  $a_0 \geq 0$  for  $f_{a_0}(a_0) = 0$  have to satisfy  $S_1(a_0) = 0$  or  $S_2(a_0) = 0$ . Since  $S_1(y_m) < 0$  implies that there is no solution satisfying  $S_2(y) = 0$ , all solutions  $a_0 \geq 0$  for  $f_{a_0}(a_0)$  have to satisfy  $S_1(a_0) = 0$  and therefore  $\frac{df_{a_0}}{da} \Big|_{a=a_0} > 0$  according to Lemma 1(3f). □

*Proof of part 2* Suppose that condition (48) is satisfied, by Lemma 1(1), we have

$$\min_{a \geq 0} f_y(a) = \gamma_1 - (\gamma_1 \gamma_3 - D)y - \frac{n-1}{n^{\frac{n}{n-1}}} \frac{(\gamma_4 + D)^{\frac{n}{n-1}}}{\gamma_2^{\frac{1}{n-1}}} (1 - \gamma_3 y)^{-\frac{1}{n-1}}.$$

If  $0 < \gamma_3 y < 1 - \frac{(n-1)^{\frac{n-1}{n}}}{n} \frac{\gamma_4 + D}{\gamma_2^{\frac{1}{n}} \gamma_1^{\frac{n-1}{n}}}$ , we have

$$\gamma_1 (1 - \gamma_3 y)^{\frac{n}{n-1}} > \frac{n-1}{n^{\frac{n}{n-1}}} \frac{(\gamma_4 + D)^{\frac{n}{n-1}}}{\gamma_2^{\frac{1}{n-1}}},$$

and therefore

$$\gamma_1 - (\gamma_1\gamma_3 - D)y > \frac{n-1}{n^{\frac{n}{n-1}}} \frac{(\gamma_4 + D)^{\frac{n}{n-1}}}{\gamma_2^{\frac{1}{n-1}}} (1 - \gamma_3 y)^{-\frac{1}{n-1}},$$

$$\min_{a \geq 0} f_y(a) > 0.$$

□

Lemma 1(3a) implies that  $y_m$  is larger than  $\frac{1}{\gamma_3} \left( 1 - \frac{(n-1)^{\frac{n-1}{n}}}{n} \frac{\gamma_4 + D}{\gamma_2^{\frac{1}{n}} \gamma_1^{\frac{n-1}{n}}} \right)$ , that is,

$$y_m > \frac{1}{\gamma_3} \left( 1 - \frac{(n-1)^{\frac{n-1}{n}}}{n} \frac{\gamma_4 + D}{\gamma_2^{\frac{1}{n}} \gamma_1^{\frac{n-1}{n}}} \right) > 0. \tag{49}$$

Then we apply Lemma 1(3h) to show that there is no solution with  $a \geq 0$  such that  $f_0(a) = 0$ .

By Lemma 1(3b, h), we know that  $(y_m, a_1(y_m))$  satisfies the following two equations:

$$f_{y_m}(a_m) = (\gamma_1 + \gamma_2 a_m^n)(1 - \gamma_3 y_m) - \gamma_4 a_m - D(a_m - y_m) = 0, \tag{50}$$

$$\frac{df_{y_m}}{da} \Big|_{a=a_m} = n\gamma_2 a_m^{n-1}(1 - \gamma_3 y_m) - \gamma_4 - D = 0, \tag{51}$$

where  $a_m = a_1(y_m)$ .

After multiplying (50) and (51) by  $n$  and  $a_m$ , respectively, we have

$$n\gamma_1(1 - \gamma_3 y_m) + n\gamma_2 a_m^n(1 - \gamma_3 y_m) - n\gamma_4 a_m - nDa_m + nDy_m = 0, \tag{52}$$

$$n\gamma_2 a_m^n(1 - \gamma_3 y_m) - \gamma_4 a_m - Da_m = 0. \tag{53}$$

Subtracting (52) by (53), we obtain

$$n\gamma_1(1 - \gamma_3 y_m) - (n-1)(\gamma_4 + D)a_m + nDy_m = 0,$$

which leads to

$$a_m = \frac{n}{n-1} \frac{1}{\gamma_4 + D} (\gamma_1 - (\gamma_3\gamma_1 - D)y_m). \tag{54}$$

By substituting (54) into  $S_1(y_m)$ , we obtain

$$S_1(y_m) = a_m - y_m = \frac{n}{n-1} \frac{1}{\gamma_4 + D} \left( \gamma_1 - \left( \gamma_1\gamma_3 - \frac{1}{n}D + \frac{n-1}{n}\gamma_4 \right) y_m \right). \tag{55}$$



By applying (49) and condition (48),

$$y_m > \frac{1}{\gamma_3} \left( 1 - \frac{(n-1)^{\frac{n-1}{n}}}{n} \frac{\gamma_4 + D}{\gamma_2^{\frac{1}{n}} \gamma_1^{\frac{n-1}{n}}} \right) > \frac{\gamma_1}{\gamma_1 \gamma_3 - \frac{1}{n} D + \frac{n-1}{n} \gamma_4},$$

which, coupled with (55), implies that  $S_1(y_m) < 0$ .

**Lemma 3** Suppose  $D = 0$ , and if

$$\left( 1 - \frac{(n-1)^{\frac{n-1}{n}}}{n} \frac{\gamma_4}{\gamma_2^{\frac{1}{n}} \gamma_1^{\frac{n-1}{n}}} \right) < \frac{\gamma_1 \gamma_3}{\gamma_1 \gamma_3 + \frac{n-1}{n} \gamma_4}. \tag{56}$$

holds, then there exists a solution  $a_0$  satisfying  $f_{a_0}(a_0) = 0$  and  $\frac{df_{a_0}}{da} \Big|_{a=a_0} < 0$ .

*Proof* There are two parts in the proof:

1. Prove that if  $S_2(y_m) \geq 0$ , there exists  $a_0 \geq 0$  such that  $f_{a_0}(a_0) = 0$  and  $\frac{df_{a_0}}{da} \Big|_{a=a_0} < 0$ .
2. Prove that condition (56) implies  $S_2(y_m) \geq 0$ .

By combining these two results, we can prove that if the condition (56) is satisfied, there exists  $a_0 \geq 0$  satisfying  $f_{a_0}(a_0) = 0$  and  $\frac{df_{a_0}}{da} \Big|_{a=a_0} < 0$ .

*Proof of part 1* Suppose  $S_2(y_m) > 0$ , as we know that  $S_2(1/\gamma_3) = -1/\gamma_3 < 0$ , then by the intermediate value theorem, there exists a solution  $a_0$  satisfying  $S_2(a_0) = 0$  ( $f_{a_0}(a_0) = 0$ ), and therefore  $\frac{df_{a_0}}{da} \Big|_{a=a_0} < 0$ , according to Lemma 1(3f).

*Proof of part 2* Suppose that condition (56) is satisfied.

If  $y_m = 0$ , we have  $S_2(y_m) = a_2(y_m) \geq 0$ , which completes the proof of part 2. Otherwise if  $y_m > 0$ , by Lemma 1(1), we have

$$\min_{a \geq 0} f_y(a) = \gamma_1 - \gamma_1 \gamma_3 y - \frac{n-1}{n^{\frac{n}{n-1}}} \frac{\gamma_4^{\frac{n}{n-1}}}{\gamma_2^{\frac{1}{n-1}}} (1 - \gamma_3 y)^{-\frac{1}{n-1}}.$$

If  $\gamma_3 y > 1 - \frac{(n-1)^{\frac{n-1}{n}}}{n} \frac{\gamma_4}{\gamma_2^{\frac{1}{n}} \gamma_1^{\frac{n-1}{n}}}$ , we have

$$\gamma_1 (1 - \gamma_3 y)^{\frac{n}{n-1}} < \frac{n-1}{n^{\frac{n}{n-1}}} \frac{\gamma_4^{\frac{n}{n-1}}}{\gamma_2^{\frac{1}{n-1}}},$$

and therefore

$$\gamma_1 - \gamma_1 \gamma_3 y < \frac{n-1}{n^{\frac{n-1}{n-1}}} \frac{\gamma_4^{\frac{n}{n-1}}}{\gamma_2^{\frac{1}{n-1}}} (1 - \gamma_3 y)^{-\frac{1}{n-1}},$$

$$\min_{a \geq 0} f_y(a) < 0.$$

Lemma 1(3h) implies that

$$y_m \leq \frac{1}{\gamma_3} \left( 1 - \frac{(n-1)^{\frac{n-1}{n}}}{n} \frac{\gamma_4}{\gamma_2^{\frac{1}{n}} \gamma_1^{\frac{n-1}{n}}} \right). \quad (57)$$

By Lemma 1(3b, h),  $(y_m, a_1(y_m))$  satisfies the following two equations:

$$f_{y_m}(a_m) = (\gamma_1 + \gamma_2 a_m^n)(1 - \gamma_3 y_m) - \gamma_4 a_m = 0, \quad (58)$$

$$\frac{df_{y_m}}{da} \Big|_{a=a_m} = n\gamma_2 a_m^{n-1} (1 - \gamma_3 y_m) - \gamma_4 = 0, \quad (59)$$

where  $a_m = a_2(y_m)$ .

After multiplying (58) and (59) by  $n$  and  $a_m$ , respectively, we have

$$n\gamma_1(1 - \gamma_3 y_m) + n\gamma_2 a_m^n (1 - \gamma_3 y_m) - n\gamma_4 a_m = 0, \quad (60)$$

$$n\gamma_2 a_m^n (1 - \gamma_3 y_m) - \gamma_4 a_m = 0. \quad (61)$$

Then subtracting (60) by (61), one obtains

$$n\gamma_1(1 - \gamma_3 y_m) - (n-1)\gamma_4 a_m = 0,$$

which leads to

$$a_m = \frac{n}{n-1} \frac{1}{\gamma_4} (\gamma_1 - \gamma_3 \gamma_1 y_m). \quad (62)$$

After substituting (62) into  $S_2(y_m)$ , we get

$$S_2(y_m) = a_m - y_m = \frac{n}{n-1} \frac{1}{\gamma_4 + D} \left( \gamma_1 - \left( \gamma_1 \gamma_3 + \frac{n-1}{n} \gamma_4 \right) y_m \right). \quad (63)$$

By applying (57) and condition (56),

$$y_m \leq \frac{1}{\gamma_3} \left( 1 - \frac{(n-1)^{\frac{n-1}{n}}}{n} \frac{\gamma_4}{\gamma_2^{\frac{1}{n}} \gamma_1^{\frac{n-1}{n}}} \right)$$

$$< \frac{\gamma_1}{\gamma_1 \gamma_3 + \frac{n-1}{n} \gamma_4},$$

which, coupled with (63), implies that  $S_2(y_m) \geq 0$ .

7.2 Proofs of Theorems 1–4

7.2.1 Theorem 1

*Proof* First, we set  $\gamma_1 = k_3$ ,  $\gamma_2 = k_4$ ,  $\gamma_3 = 1$ ,  $\gamma_4 = k_{\text{off}}$ , and  $D = D^*$  in the lemmas. By applying Lemma 2, we obtain that if

$$1 - \frac{(n - 1) \frac{n-1}{n} k_{\text{off}} + D^*}{n \frac{k_4^{\frac{1}{n}} k_3^{\frac{n-1}{n}}}{k_4^{\frac{1}{n}} k_3^{\frac{n-1}{n}}}} > \frac{k_3}{k_3 - \frac{1}{n} D^* + \frac{n-1}{n} k_{\text{off}}} \tag{64}$$

then

$$nk_4 a_0^{n-1} (1 - a_0) - k_{\text{off}} - D^* > 0 \tag{65}$$

holds for any  $a_0$  satisfying

$$(k_3 + k_4 a_0^n)(1 - a_0) - k_{\text{off}} a_0 = 0. \tag{66}$$

By (30), we know that  $a_0$  is a homogeneous steady state solution for  $a$  in system (1)–(2) with the cooperative feedback (28) if and only if  $a_0$  satisfies (66). Also, by  $D^* > \sigma_1 D_m + \frac{\sigma_1 D_m}{\sigma_1 D_m + g_{\text{off}}}(k_{11} + k_{12} a_0)$ , inequality (65) implies inequality (26).

By the result obtained from Lemma 2, we have proved that if (64) is satisfied, then all possible homogeneous steady state solutions satisfy inequality (26). Since at least one homogeneous steady state solution satisfies inequality (25), we have proved that if

$$1 - \frac{(n - 1) \frac{n-1}{n} k_{\text{off}} + D^*}{n \frac{k_4^{\frac{1}{n}} k_3^{\frac{n-1}{n}}}{k_4^{\frac{1}{n}} k_3^{\frac{n-1}{n}}}} > \frac{k_3}{k_3 - \frac{1}{n} D^* + \frac{n-1}{n} k_{\text{off}}}$$

then there exists a homogeneous steady state solution satisfying (25) and (26). In addition, since all possible homogeneous steady state solutions satisfy inequality (26) in this case, locally stable homogeneous steady state solution does not exist.  $\square$

7.2.2 Theorem 2

*Proof* Let  $\gamma_1 = k_3$ ,  $\gamma_2 = k_4$ ,  $\gamma_3 = 1$ ,  $\gamma_4 = k_{\text{off}}$ , and  $D = 0$  in the lemmas. By applying Lemma 3, we obtain that if

$$1 - \frac{(n - 1) \frac{n-1}{n} k_{\text{off}}}{n \frac{k_4^{\frac{1}{n}} k_3^{\frac{n-1}{n}}}{k_4^{\frac{1}{n}} k_3^{\frac{n-1}{n}}}} < \frac{k_3}{k_3 + \frac{n-1}{n} k_{\text{off}}},$$

there exists a solution  $a_0$  satisfying

$$(k_3 + k_4 a_0^n)(1 - a_0) - k_{\text{off}} a_0 = 0$$

and

$$nk_4a_0^{n-1}(1 - a_0) - k_{\text{off}} < 0. \tag{67}$$

By (30), we know that  $a_0$  is a homogeneous steady state solution for  $a$  in the system (1)–(2) with the cooperative feedback (28) if and only if  $a_0$  satisfies (66). Also, inequality (67) implies that a homogeneous steady state solution is locally stable for perturbations with any nonnegative wavenumber [satisfying the condition (25) but not satisfying (26)]. So we have proved that if the condition

$$1 - \frac{(n - 1)^{\frac{n-1}{n}}}{n} \frac{k_{\text{off}}}{k_4^{\frac{1}{n}} k_3^{\frac{n-1}{n}}} < \frac{k_3}{k_3 + \frac{n-1}{n} k_{\text{off}}}$$

is satisfied, there exists a locally stable homogeneous steady state solution. □

### 7.2.3 Theorem 3

*Proof* First, we set  $\gamma_1 = k_5$ ,  $\gamma_2 = k_6$ ,  $\gamma_3 = \frac{k_{\text{on}}^* + k_{\text{off}}}{k_{\text{on}}^*}$ ,  $\gamma_4 = k_{\text{off}}$  and  $D = D^+$  in the lemmas. By applying Lemma 2, we obtain that if

$$1 - \frac{(n - 1)^{\frac{n-1}{n}}}{n} \frac{k_{\text{off}} + D^*}{k_6^{\frac{1}{n}} k_5^{\frac{n-1}{n}}} > \frac{\frac{k_{\text{on}}^* + k_{\text{off}}}{k_{\text{on}}^*} k_5}{\frac{k_{\text{on}}^* + k_{\text{off}}}{k_{\text{on}}^*} k_5 - \frac{1}{n} D^+ + \frac{n-1}{n} k_{\text{off}}}, \tag{68}$$

then

$$nk_6a_0^{n-1} \left( 1 - \frac{k_{\text{on}}^* + k_{\text{off}}}{k_{\text{on}}^*} a_0 \right) - k_{\text{off}} - D^+ > 0 \tag{69}$$

holds for any  $a_0$  satisfying

$$(k_5 + k_6a_0^n) \left( 1 - \frac{k_{\text{on}}^* + k_{\text{off}}}{k_{\text{on}}^*} a_0 \right) - k_{\text{off}}a_0 = 0. \tag{70}$$

By (41), we know that  $a_0$  is a homogeneous steady state solution for  $a$  in the system (1)–(2) with the feedback form (39) if and only if  $a_0$  satisfies (69).

By equation (70) with  $k_5 = k_{21}k_{\text{on}}^*$  and  $k_6 = k_{22}k_{\text{on}}^*$ , we have

$$1 + k_{21} + k_{22}a_0^n = \frac{1 - a_0}{1 - \frac{k_{\text{on}}^* + k_{\text{off}}}{k_{\text{on}}^*} a_0}. \tag{71}$$

Now we substitute the feedback form (39) into inequality (26), we obtain

$$-\sigma_1 D_m + \frac{nk_6a_0^{n-1}}{1 + k_{21} + k_{22}a_0^n} (1 - a_0) - k_{\text{off}} - \frac{\sigma_1 D_m}{\sigma_1 D_m + g_{\text{off}}} k_{\text{on}} \frac{k_{21} + k_{22}a_0^n}{1 + k_{21} + k_{22}a_0^n} > 0,$$

and by using (71), this inequality can be rewritten as

$$\begin{aligned}
 & -\sigma_1 D_m + nk_6 a_0^{n-1} \left( 1 - \frac{k_{on}^* + k_{off}}{k_{on}^*} a_0 \right) \\
 & -k_{off} - \frac{\sigma_1 D_m}{\sigma_1 D_m + g_{off}} k_{on} \frac{k_{21} + k_{22} a_0^n}{1 + k_{21} + k_{22} a_0^n} > 0.
 \end{aligned}$$

Since  $D^+ > \sigma_1 D_m + \frac{\sigma_1 D_m}{\sigma_1 D_m + g_{off}} \frac{k_{21} + k_{22} a_0^n}{1 + k_{21} + k_{22} a_0^n}$ , inequality (69) implies inequality (26).

By the result obtained from Lemma 2, we have proved that if (68) is satisfied, then all possible homogeneous steady state solutions satisfy inequality (26). Since at least one homogeneous steady state solution satisfies (25), we have proved that if

$$1 - \frac{(n-1) \frac{n-1}{n} k_{off} + D^*}{n \frac{1}{k_6^n} k_5^{\frac{n-1}{n}}} > \frac{k_5}{k_5 - \frac{1}{n} \frac{k_{on}^*}{k_{on}^* + k_{off}} D^+ + \frac{n-1}{n} \frac{k_{on}^*}{k_{on}^* + k_{off}} k_{off}},$$

there exists a homogeneous steady state solution satisfying (25) and (26). In addition, since all possible homogeneous steady state solutions satisfy (26) in this case, locally stable homogeneous steady state solution does not exist. □

7.2.4 Theorem 4

*Proof* Let  $\gamma_1 = k_5$ ,  $\gamma_2 = k_6$ ,  $\gamma_3 = \frac{k_{on}^* + k_{off}}{k_{on}^*}$ ,  $\gamma_4 = k_{off}$  and  $D = 0$  in the lemmas. By applying Lemma 3, we obtain that if

$$1 - \frac{(n-1) \frac{n-1}{n} k_{off}}{n \frac{1}{k_6^n} k_5^{\frac{n-1}{n}}} < \frac{k_5}{k_5 + \frac{n-1}{n} \frac{k_{on}^*}{k_{on}^* + k_{off}} k_{off}},$$

then there exists a solution  $a_0$  satisfying

$$(k_5 + k_6 a_0^n) \left( 1 - \frac{k_{on}^* + k_{off}}{k_{on}^*} a_0 \right) - k_{off} a_0 = 0$$

and

$$nk_6 a_0^{n-1} \left( 1 - \frac{k_{on}^* + k_{off}}{k_{on}^*} a_0 \right) - k_{off} < 0. \tag{72}$$

By (41), we know that  $a_0$  is a homogeneous steady state solution for  $a$  in the system (1)–(2) with the feedback form (39) if and only if  $a_0$  satisfies (69).

By (71), (72) can be written as

$$\frac{nk_6 a_0^{n-1}}{1 + k_{21} + k_{22} a_0^n} (1 - a_0) - k_{off} < 0,$$

which implies that a homogeneous steady state solution is locally stable for perturbations with any nonnegative wavenumber (satisfying the condition (25) but not (26)). Thus, we have proved that if the condition

$$1 - \frac{(n-1) \frac{n-1}{n} k_{\text{off}}}{n \frac{1}{k_6^n} k_5^{\frac{n-1}{n}}} < \frac{k_5}{k_5 + \frac{n-1}{n} \frac{k_{\text{on}}^*}{k_{\text{on}}^* + k_{\text{off}}} k_{\text{off}}}$$

is satisfied, there exists a locally stable homogeneous steady state solution.  $\square$

## References

- Altschuler SJ, Angenent SB, Wang Y, Wu LF (2008) On the spontaneous emergence of cell polarity. *Nature* 454(7206):886–889. doi:[10.1038/nature07119](https://doi.org/10.1038/nature07119)
- Bryant DM, Mostov KE (2008) From cells to organs: building polarized tissue. *Nat Rev Mol Cell Biol* 9(11):887–901. doi:[10.1038/nrm2523](https://doi.org/10.1038/nrm2523)
- Drubin DG, Nelson WJ (1996) Origins of cell polarity. *Cell* 84:335–344
- Freisinger T, Klunder B, Johnson J, Muller N, Pichler G, Beck G, Costanzo M, Boone C, Cerione RA, Frey E, Wedlich-Soldner R (2013) Establishment of a robust single axis of cell polarity by coupling multiple positive feedback loops. *Nat Commun* 4:1807. doi:[10.1038/ncomms2795](https://doi.org/10.1038/ncomms2795)
- Goldstein B, Macara IG (2007) The par proteins: fundamental players in animal cell polarization. *Dev Cell* 13(5):609–622. doi:[10.1016/j.devcel.2007.10.007](https://doi.org/10.1016/j.devcel.2007.10.007)
- Goryachev AB, Pokhilko AV (2008) Dynamics of Cdc42 network embodies a Turing-type mechanism of yeast cell polarity. *FEBS Lett* 582(10):1437–1443. doi:[10.1016/j.febslet.2008.03.029](https://doi.org/10.1016/j.febslet.2008.03.029)
- Humbert P, Russell S, Richardson H (2003) Dlg, scribble and lgl in cell polarity, cell proliferation and cancer. *Bioessays* 25(6):542–553. doi:[10.1002/bies.10286](https://doi.org/10.1002/bies.10286)
- Jilkine A, Edelstein-Keshet L (2011) A comparison of mathematical models for polarization of single eukaryotic cells in response to guided cues. *PLoS Comput Biol* 7(4):e1001121. doi:[10.1371/journal.pcbi.1001121](https://doi.org/10.1371/journal.pcbi.1001121)
- Jilkine A, Maree AFM, Edelstein-Keshet L (2007) Mathematical model for spatial segregation of the Rho-family GTPases based on inhibitory crosstalk. *Bull Math Biol* 69(6):1943–1978. doi:[10.1007/s11538-007-9200-6](https://doi.org/10.1007/s11538-007-9200-6)
- Krahn MP, Wodarz A (2012) Phosphoinositide lipids and cell polarity: linking the plasma membrane to the cytoskeleton. *Essays Biochem* 53:15–27. doi:[10.1042/bse0530015](https://doi.org/10.1042/bse0530015)
- Levine H, Rappel W-J (2005) Membrane-bound Turing patterns. *Phys Rev E* 72(6 Pt 1):061912
- Lo W-C, Lee ME, Narayan M, Chou C-S, Park H-O (2013) Polarization of diploid daughter cells directed by spatial cues and GTP hydrolysis of Cdc42 in budding yeast. *PLoS One* 8(2):e56665. doi:[10.1371/journal.pone.0056665](https://doi.org/10.1371/journal.pone.0056665)
- Maree AFM, Jilkine A, Dawes A, Grieneisen VA, Edelstein-Keshet L (2006) Polarization and movement of keratocytes: a multiscale modelling approach. *Bull Math Biol* 68(5):1169–1211. doi:[10.1007/s11538-006-9131-7](https://doi.org/10.1007/s11538-006-9131-7)
- Marth W, Voigt A (2014) Signaling networks and cell motility: a computational approach using a phase field description. *J Math Biol* 69(1):91–112
- Meinhardt H (1982) *Models of biological pattern formation*. Academic Press, London
- Moore T, Chou C-S, Nie Q, Joen NL, Yi T-M (2008) Robust spatial sensing of mating pheromone gradients by yeast cells. *PLoS One* 3(12):e38865
- Park H-O, Bi E (2007) Central roles of small GTPases in the development of cell polarity in yeast and beyond. *Microbiol Mol Biol Rev* 71(1):48–96. doi:[10.1128/MMBR.00028-06](https://doi.org/10.1128/MMBR.00028-06)
- Raftopoulou M, Hall A (2004) Cell migration: Rho GTPases lead the way. *Dev Biol* 265(1):23–32
- Rätz A, Röger M (2012) Turing instabilities in a mathematical model for signaling networks. *J Math Biol* 65(6–7):1215–1244. doi:[10.1007/s00285-011-0495-4](https://doi.org/10.1007/s00285-011-0495-4)
- Rätz A, Röger M (2013) Symmetry breaking in a bulk-surface reaction-diffusion model for signaling networks. <http://arxiv.org/abs/13056172v1>

- Rubinstein B, Slaughter BD, Li R (2012) Weakly nonlinear analysis of symmetry breaking in cell polarity models. *Phys Biol* 9(4):045,006. doi:[10.1088/1478-3975/9/4/045006](https://doi.org/10.1088/1478-3975/9/4/045006)
- Slaughter BD, Smith SE, Li R (2009) Symmetry breaking in the life cycle of the budding yeast. *Cold Spring Harb Perspect Biol* 1(a003):384
- Smith SE, Rubinstein B, Mendes Pinto I, Slaughter BD, Unruh JR, Li R (2013) Independence of symmetry breaking on Bem1-mediated autocatalytic activation of Cdc42. *J Cell Biol* 202(7):1091–1106
- Turing AM (1990) The chemical basis of morphogenesis. 1953. *Bull Math Biol* 52(1–2):153–197
- Wedlich-Soldner R, Li R (2003) Spontaneous cell polarization: undermining determinism. *Nat Cell Biol* 5:267–270